A dual function of SnRK2 kinases in the regulation of SnRK1 and plant growth

Borja Belda-Palazón[1,2,6], Mattia Adamo[1,5,6], Concetta Valerio[1,6], Liliana Ferreira[1], Ana Confraria[1], Diana Reis-Barata[1], Américo Rodrigues[3§], Christian Meyer[4], Pedro L. Rodriguez[2], and Elena Baena-González[1,*]

[1]Instituto Gulbenkian de Ciência, 2780-156 Oeiras, Portugal and GREEN-IT Bioresources for Sustainability, ITQB NOVA, 2780-157 Oeiras, Portugal

[2]Instituto de Biología Molecular y Celular de Plantas, Consejo Superior de Investigaciones Científicas–Universidad Politécnica de Valencia, 46022 Valencia, Spain

[3]MARE Marine and Environmental Sciences Centre, ESTM, Instituto Politécnico de Leiria, 2520-641 Peniche, Portugal

[4]Institut Jean-Pierre Bourgin (IJPB), INRAE, AgroParisTech, Université Paris-Saclay, 78000 Versailles, France

[5]Current address: BPMP, Univ Montpellier, CNRS, INRA, Montpellier SupAgro, 34090 Montpellier, France

[6]These authors contributed equally to the work

[§] Deceased

[*]Corresponding author. Instituto Gulbenkian de Ciência, Rua da Quinta Grande 6, 2780-156 Oeiras, Portugal. Tel.: +351 214464630; Fax: +351 214407970; e-mail: ebaena@igc.gulbenkian.pt

Keywords: *growth regulation, abscisic acid, energy signaling, SnRK1, TOR, Arabidopsis thaliana*

Adverse environmental conditions trigger responses in plants that promote stress tolerance and survival at the expense of growth[1]. However, little is known of how stress signaling pathways interact with each other and with growth regulatory components to balance growth and stress responses. Here, we show that plant growth is largely regulated by the interplay between the evolutionarily conserved energy-sensing AMPK/SnRK1 protein kinase and the ABA (abscisic acid) phytohormone pathway. While SnRK2 kinases are major drivers of ABA-triggered stress responses, we uncover an unexpected growth-promoting function of these kinases in the absence of ABA as repressors of SnRK1. Sequestration of SnRK1 by SnRK2-containing complexes inhibits SnRK1 signaling, thereby allowing TOR activity and growth under optimal conditions. On the other hand, these complexes are essential for releasing and activating SnRK1 in response to ABA, leading to the inhibition of TOR and growth under stress. This dual regulation of SnRK1 by SnRK2 kinases couples growth control with environmental factors typical for the terrestrial habitat and is likely to have been critical for the water-to-land transition of plants.

To cope with adverse environmental conditions, plants trigger cellular and whole-plant responses that confer protection but are often detrimental to growth[1]. Despite the negative impact of stress on crop productivity, how growth is modified by stress signalling pathways is poorly understood. One major component of the stress response is SNF1-related protein kinase 1 (SnRK1), the plant ortholog of yeast SNF1 (Sucrose non-fermenting 1) and mammalian AMPK (AMP-activated protein Kinase), which drives vast metabolic and transcriptional readjustments that restore homeostasis and promote survival[2-4]. Similarly to SNF1 and AMPK, SnRK1 signaling is activated when energy levels decline during stress[2], but is also induced by abscisic acid (ABA)[5], a phytohormone essential for responses to stresses like drought, extreme temperatures or salinity[6]. In the absence of ABA, type 2C phosphatases (PP2Cs) repress subgroup III SnRK2 kinases (SnRK2.2, SnRK2.3, and SnRK2.6 in *Arabidopsis thaliana*), keeping the pathway inactive[7-11]. Binding of ABA to its receptors enables PP2C sequestration and the release and activation of SnRK2s, which thereby induce protective responses and inhibit growth[12,13].

Numerous studies have suggested cooperation between SnRK1 and ABA signaling in plant stress responses, growth and development[5,14-22], but little is known of the underlying mechanisms. SnRK1 is a heterotrimeric complex and in Arabidopsis the α-catalytic subunit is encoded by two genes, *SnRK1α1* and *SnRK1α2*. To investigate the molecular connection

between SnRK1 and ABA signaling and, given the lethality of the double *snrk1α1 snrk1α2* knockout[2,23], we generated partial *snrk1α1*$^{-/-}$ *snrk1α2*$^{+/-}$ loss-of-function mutants. These mutants show compromised SnRK1 accumulation (Supplementary Fig. 1) and signaling (Supplementary Fig. 2), as demonstrated by defective induction of SnRK1 marker genes in response to a transient dark treatment[2]. These are hereafter referred as *sesquiα2-1* or *sesquiα2-2* mutants, depending on the *snrk1α2* allele they harbor.

Despite being mostly similar to the wild-type during early development under normal conditions, *sesquiα2* mutants fail to impose an ABA-dependent post-germination growth arrest[24], developing green cotyledons in the presence of the hormone (Fig. 1a, Supplementary Fig. 3). Furthermore, *sesquiα2* mutants are unable to reduce lateral root (LR) number in response to ABA to the same extent as control plants (10%, 55%, and 41% of the mock for WT, *sesquiα2-1,* and *sesquiα2-2* seedlings, respectively; Fig. 1b). In similar assays, single *snrk1α1* and *snrk1α2* mutants are mostly indistinguishable from the wild-type, with only the *snrk1α1* mutant being mildly defective in the repression of LR growth in response to ABA (Supplementary Fig. 4). Other ABA-regulated processes, such as germination (Supplementary Fig. 5a), primary root (PR) growth (Fig. 1b), transpiration rates (Supplementary Fig. 5b), and ABA marker gene induction (Supplementary Fig. 5c) appeared normal in *sesquiα2* mutants, suggesting that the lack of SnRK1 affects only specific ABA responses and/or that SnRK1 signaling is not sufficiently compromised to visibly affect all ABA-related processes. Importantly, *sesquiα2* mutants fail to repress LR growth also under low light conditions (Supplementary Fig. 6), showing that defective growth inhibition is not exclusive to ABA, and that, given the weak nature of this mutant, its defects are only apparent under conditions that substantially compromise growth in WT plants.

Given that all the observed ABA phenotypes of the SnRK1 *sesquiα2* mutants relate to growth repression, and given the known antagonistic relationship between AMPK/SnRK1 and the growth-promoting Target of Rapamycin (TOR) kinase in animals[25] and possibly in plants[4], we examined the activation status of TOR in the *sesquiα2-1* mutant in response to ABA. The phosphorylation of ribosomal protein S6 (RPS6^{S240}) in whole seedling extracts served as a faithful readout[26], confirming previous results on the inhibition of TOR signaling by ABA and its dependency on SnRK2 kinases[27] (Supplementary Fig. 7). In response to ABA, the *sesquiα2-1* mutant showed a slower inhibition of TOR along all the analyzed 4h time-course sampling points (Fig. 1c), indicating that SnRK1α1 is required for repressing TOR activity in response to ABA. To assess if the SnRK1α effect is direct, we next analyzed the physical interaction

between SnRK1α1 and TOR by co-immunoprecipitation (co-IP), using a GFP-tagged SnRK1α1 line[14], a *35S::GFP* control line, and antibodies recognizing TOR or its regulatory protein RAPTOR. In whole seedling extracts TOR was readily co-immunoprecipitated with SnRK1α1-GFP (Fig. 1d) but not with GFP alone (Fig. 1e). A basal SnRK1α1-TOR interaction was detected in mock conditions, and it was enhanced two-fold by a short ABA treatment (40 min; Fig. 1d). Similar results were obtained for RAPTOR (Supplementary Fig. 8a-b), confirming previous observations that SnRK1α1 and RAPTOR interact *in planta*[4,28]. These results were further corroborated for the endogenous proteins using TOR immunoprecipitation and immunodetection of SnRK1α1 (Supplementary Fig. 8d). A recent study demonstrated that the repression of TOR by ABA is SnRK2-dependent[27]. However, using a GFP-tagged SnRK2.2 line[29] we were unable to detect any interaction of TOR or RAPTOR with SnRK2.2-GFP either in mock- or ABA-treated plants (Fig. 1f and Supplementary Fig. 8c). Furthermore, none of the three SnRK2s (SnRK2.2/2.3/2.6) could be detected in immunoprecipitates of endogenous TOR in either of the two conditions (Supplementary Fig. 8d), altogether suggesting that, despite being necessary for repressing TOR in response to ABA[27], SnRK2s may not be directly involved in TOR repression and that TOR is instead inhibited by SnRK1.

To explore the molecular connection between SnRK2 and SnRK1, we first examined their potential co-localization. As previously reported, SnRK1α1 and SnRK2.2 were prominently expressed in the root tip, in LR primordia and in subsequent stages of LR development (Supplementary Fig. 9)[14,29]. At the subcellular level both kinases were present in the cytosol and the nucleus, being particularly enriched in the latter (Supplementary Fig. 9). To investigate the SnRK1-SnRK2 physical interaction we next performed reciprocal co-IP experiments using the same material and conditions as for the microscopy analyses (roots, 3h ABA treatment). In mock-treated seedlings we retrieved a clear interaction between SnRK1α1 and SnRK2 in both directions (Fig. 2a-2b), whilst neither SnRK2 nor SnRK1α1 could be detected in immunoprecipitates of GFP alone (Supplementary Fig. 10a). The reported interaction of both SnRK2[9,10] and SnRK1α1[5] with clade A PP2C phosphatases served as positive controls (Fig. 2c-d). Strikingly, treatment with ABA caused a marked reduction in all three interactions (Fig. 2a-d; for the PP2CA interactions please note that this is relative to the total PP2CA amount, which is known to be strongly increased by ABA through transcriptional activation[30]), suggesting that the three proteins may be part of the same complexes. A similar effect of ABA on the SnRK2-SnRK1α1 interaction was observed using the same material and conditions as for evaluating the interaction with TOR (whole seedlings, 40 min ABA treatment; Supplementary Fig. 10b-c), showing the interaction is rapidly reduced by the hormone. Using

128 seedlings overexpressing FLAG-tagged SnRK2.3 and SnRK2.6 we could further demonstrate
129 that the interaction between SnRK1α1 and SnRK2s as well as the reduction of this interaction
130 by ABA is shared by all three ABA-induced SnRK2 kinases (Supplementary Fig. 10d-e).

131 To assess whether the interaction between SnRK1 and SnRK2 is direct or whether it is
132 dependent on the presence of PP2Cs we used bimolecular fluorescence complementation
133 (BiFC) assays in *Nicotiana benthamiana* (Fig. 2e and Supplementary Fig. 11a-b). Expression
134 of YFP^N-SnRK1α1 with YFP^C-SnRK2s and a nuclear targeted RFP control (mRFP-NLS) did
135 not result in YFP reconstitution (Fig. 2e and Supplementary Fig. 11a-b). However, co-
136 expression of the two kinases with PP2CA-RFP yielded a very strong YFP signal in the nucleus,
137 indicating that the presence of PP2CA enables SnRK2s to interact with SnRK1α1. Moreover,
138 a kinase dead SnRK2.6 variant [$SnRK2.6^{G33R}$][31] was also able to interact with SnRK1α1 in a
139 PP2CA-dependent manner, demonstrating that the SnRK1α1-SnRK2 interaction does not rely
140 on the kinase activity of the latter (Supplementary Fig. 11a-b). Immunoblot analyses of the
141 infiltrated leaf sectors confirmed the expression of YFP^N-SnRK1α1 and YFP^C-SnRK2s in all
142 samples (Supplementary Fig. 11c).

143 To investigate the relationship between SnRK1 and SnRK2 kinases we crossed the
144 *snrk1α1* single mutant to the *snrk2.2/2.3* double mutant (hereafter referred as *snrk2d*) to assess
145 their genetic interaction (Supplementary Fig. 12). We reasoned that, given the partial
146 impairment of ABA responses in this mutant[7] [as opposed to the full impairment of the
147 *snrk2.2/2.3/2.6* mutant (*snrk2t*)[32-34]], a potential contribution from the *snrk1α1* mutation could
148 be more easily detected in this background. Despite having mostly no effect on its own
149 (Supplementary Fig. 4), the *snrk1α1* mutation clearly enhanced the ABA insensitivity of the
150 *snrk2d* mutant, increasing its germination and cotyledon greening rates (Fig. 3a-b), and the
151 formation of LRs in ABA (Fig. 3c). This indicates that the SnRK1 pathway contributes to
152 specific ABA signaling outputs. Furthermore, the sensitization of the *snrk1α1* mutation by the
153 *snrk2d* background in ABA, suggests that SnRK2s may promote SnRK1 signaling in these
154 conditions. To investigate whether SnRK2s can phosphorylate and activate SnRK1 directly, we
155 first immunoprecipitated active and inactive HA-tagged SnRK2.3 variants expressed in
156 Arabidopsis mesophyll protoplasts treated under mock or ABA conditions. Selective activation
157 of SnRK2.3 by ABA was validated using a *RD29B::LUC* reporter assay[35] (Supplementary Fig.
158 13a). Immunoprecipitated proteins were tested in an *in vitro* SnRK1α1 kinase assay using a
159 similarly generated SnRK1 upstream kinase (SnAK2[36]). Whilst incubation of recombinant
160 SnRK1α1 with immunoprecipitated SnAK2 resulted in a strong induction of SnRK1 activity,
161 no effect was observed for the ABA-activated SnRK2.3, which yielded similarly low SnRK1

162 activities as the inactive SnRK2.3^{K51N} variant (Supplementary Fig. 13b-c). Altogether, these
163 results suggest that SnRK2s promote SnRK1 signaling but this does not appear to involve direct
164 SnRK1α1 activation.

165 We next asked whether repression of TOR by SnRK1 always requires SnRK2s or
166 whether this requirement is specific to ABA. To address this, we compared the inhibition of
167 TOR by a dark-induced energy deficit in control plants, *sesquiα2-1*, and *snrk2t* mutants. As
168 expected, *sesquiα2-1* seedlings had a reduced capacity to repress RPS6^{S240} phosphorylation in
169 response to darkness (Supplementary Fig. 14a). This is consistent with previous reports
170 showing defective repression of TOR outputs in plants that have compromised SnRK1
171 signaling[4]. However, the *snrk2t* mutant displayed similar kinetics in the repression of TOR
172 signaling as the wild-type (Supplementary Fig. 14b), supporting the idea that SnRK2s are only
173 required for repressing TOR *via* SnRK1 in response to ABA but not energy depletion.

174 We noticed that, despite its ABA insensitivity and overall increased growth in ABA, the
175 *snrk2d* mutant displayed reduced PR and LR growth in control plates compared to the WT (Fig.
176 3c), in accordance with a previous report[29]. Most strikingly, this was fully rescued by the
177 *snrk1α1* mutation, indicating that the reduced growth of the *snrk2d* mutant is SnRK1α1-
178 dependent and suggesting that, in the absence of ABA, SnRK2s promote root growth by
179 repressing SnRK1α1 (Fig. 3c). Further supporting a growth-promoting function of SnRK2s in
180 normal conditions, a line overexpressing SnRK2.3 had longer PR in control plates
181 (Supplementary Fig. 15), whilst showing enhanced repression of PR growth in ABA, in
182 accordance with its known ABA hypersensitivity[37]. To assess whether the differences in growth
183 observed in mock conditions are TOR-dependent, we grew seedlings in increasing
184 concentrations of the TOR inhibitor AZD8055. The *snrk2d* mutant displayed a clear
185 hyposensitivity to AZD, with differences in PR length between WT and *snrk2d* seedlings being
186 strongly reduced under increasing concentrations of the inhibitor (Fig. 3d). Furthermore, a
187 normal sensitivity to AZD was restored by the *snrk1α1* mutation, indicating that the lower TOR
188 activity of the *snrk2d* mutant is SnRK1-dependent (Fig. 3d). To further explore how the
189 interplay between SnRK2 and SnRK1 kinases affects TOR activity, we performed a time-
190 course experiment to monitor the induction of RPS6 phosphorylation in response to nutrient
191 supplementation (replacement of the growth medium with fresh medium; Fig. 3e). In WT
192 seedlings a marked increase in RPS6 phosphorylation was detected within the first 30 min of
193 refreshing the medium, followed by a slight decrease and stabilization after 1h. In the *snrk2d*
194 mutant, however, the induction of RPS6 phosphorylation was defective, but this defect was
195 fully rescued by the *snrk1α1* mutation. Altogether this and the AZD sensitivity experiment

196 show that in the *snrk2d* mutant TOR is repressed to a higher extent than in WT plants and that
197 this overrepression is SnRK1-dependent. These results further suggest that in the absence of
198 SnRK2s, basal SnRK1 activity is increased. To investigate this, we analyzed WT and *snrk2d*
199 seedlings with regard to the phosphorylation status of TREHALOSE PHOSPHATE
200 SYNTHASE 5 (TPS5), a established direct target of SnRK1[38,39]. The *tps5-1* mutant is a
201 knockout for TPS5[40] and served as a control for the specificity of the TPS5 antibody (Fig. 3f).
202 We found that the levels of TPS5 phosphorylation were indeed higher in the *snrk2d* mutant
203 (1.7-fold), consistent with an enhanced SnRK1 activity. To explore this further we
204 immunoprecipitated SnRK1α1 from WT and *snrk2d* seedlings and analyzed its interaction with
205 the SnRK1β1 regulatory subunit. The β-regulatory subunits are considered to act as scaffolds
206 in the SnRK1 complex, being crucial for the recruitment of specific targets[41]. The SnRK1β1
207 subunit, in particular, has been implicated in the control of nitrogen and carbon metabolism[42]
208 and we therefore reasoned it could be involved in the regulation of TOR and TPS5 by the
209 SnRK1 complex. The interaction of SnRK1α1 with the SnRK1β1 subunit was indeed higher
210 (1.7-fold) in the *snrk2d* mutant (Fig. 3g), suggesting that the lower TOR activity and increased
211 TPS5 phosphorylation of this mutant could be the result of enhanced engagement of the
212 SnRK1β1 subunit.

213 We conclude that SnRK2 kinases perform dual functions in plants (Fig. 4). In the
214 absence of ABA, SnRK2s promote growth: SnRK2s are required, together with PP2Cs, to form
215 "repressor complexes" that sequester SnRK1, precluding its interaction with TOR and thereby
216 the inhibition of TOR signaling and growth. Sequestration of SnRK1α1 in these complexes is
217 important for root growth (in the case of SnRK2.2 and SnRK2.3), and may potentially explain
218 other reported unexpected effects of SnRK2 kinases, including SnRK2.6, in promoting
219 metabolism, growth, and development in optimal conditions[43,44]. We propose that these
220 complexes are the same as the ones performing canonical ABA signaling functions and that
221 their disassembly requires sequestration of the PP2C repressors by the ABA-bound ABA
222 receptors. Several lines of evidence support this. First, likewise SnRK2s[45], the activation of
223 SnRK1 by ABA requires relief of inhibition by PP2C phosphatases[5]. Second, ABA reduces the
224 interaction of SnRK1α1 with SnRK2 and PP2CA and between SnRK2 and PP2CA (Figs 2a-d,
225 Supplementary Fig. 10b-c). Third, SnRK1α1 and SnRK2 are unable to interact in the absence
226 of PP2Cs (Fig. 2e). Forth, SnRK2s (SnRK2.2/SnRK2.3/SnRK2.6) are absolutely required for
227 repressing TOR in response to ABA[27] (Supplementary Fig. 7b), even though SnRK2s may be
228 involved in TOR repression only indirectly.

229 In the presence of ABA, SnRK2s repress growth and this is partly accomplished by
230 enabling SnRK1 activation by the hormone (Fig. 4): SnRK1 repressor complexes harboring
231 SnRK2s and PP2Cs dissociate through canonical ABA signaling, releasing SnRK1α1 and
232 SnRK2 to activate stress responses. One major consequence of the ABA-triggered disassembly
233 of these complexes is the interaction of released SnRK1α1 with TOR, ultimately leading to
234 growth inhibition. In the absence of SnRK2s these repressor complexes are not formed,
235 rendering SnRK1 and the repression of TOR insensitive to ABA. In agreement with this,
236 Arabidopsis *raptor and lst8* mutants are ABA hypersensitive with regard to germination, early
237 seedling development, and root growth[46,47] whilst TOR overexpressors in rice display ABA
238 insensitivity during germination[48]. The fact that the ABA sensitivity of the *sesquiα2* mutants
239 was only manifested at the level of cotyledon greening and LR density but not at the level of
240 germination or PR length (Fig. 1), is likely to be explained by the weak nature of these mutants
241 (Supplementary Fig. 2), by the fact that germination had to be scored from a segregating seed
242 population and by the fact that LRs are more sensitive to ABA than the PR[49]. Repression of
243 TOR in response to ABA may also require active input from SnRK2[27]. However, given the lack
244 of interaction between SnRK2s and TOR *in planta* (Fig. 1f and Supplementary Fig. 8), the
245 simple requirement of SnRK2s to form SnRK1 repressor complexes that disassemble in
246 response to ABA may be sufficient to explain why SnRK2s are essential for growth repression
247 by this hormone[27].

248 Repression of SnRK1 by SnRK2 and PP2C allows SnRK1 to be released and activated
249 in response to ABA. However, SnRK1 is also regulated by energy depletion through
250 mechanisms that are SnRK2-independent (Supplementary Fig. 14), suggesting that SnRK1
251 associates with different factors that enable its activation in response to specific signals. We
252 propose that, in addition to its ancient and highly conserved energy-sensing function, SnRK1
253 evolved in land plants to respond to ABA, a crucial signal for survival in terrestrial habitats.
254 Intriguingly, this is accomplished through repression by the phylogenetically related subgroup
255 III SnRK2 kinases, which belong to the same SnRK superfamily as SnRK1[50], but are specific
256 to land plants[51,52]. Coupling the ABA-PP2C-SnRK2 module to the evolutionarily conserved
257 SnRK1-TOR axis conferred plants the capacity to regulate growth in response to water
258 availability and may have represented a steppingstone for the establishment of terrestrial life.

259

260 **MATERIALS AND METHODS**

261 A list of all primers, antibodies, and plant lines used in this study is provided in Table S1.
262
263 **Plant material and growth**
264 All *Arabidopsis thaliana* plants used in this study are in the Columbia (Col-0) background.
265 Unless otherwise specified, plants were grown under long-day conditions (16h light, 100 µmol
266 $m^{-2}s^{-1}$, 22°C /8h dark, 18°C) on 0.5X MS medium (0.05% MES and 0.8% phytoagar). The
267 *sesquiα2-1* (*snrk1α1-3*$^{-/-}$ *snrk1α2-1*$^{+/-}$) and *sesquiα2-2* (*snrk1α1-3*$^{-/-}$ *snrk1α2-2*$^{+/-}$) mutants were
268 obtained by crossing the *snrk1α1-3* (GABI_579E09) with the *snrk1α2-1* (WiscDsLox320B03)
269 and *snrk1α2-2* (WiscDsLox384F5) mutants, respectively. *sesquiα2* individuals were always
270 pre-selected on BASTA-containing medium for 5-6 days together with a BASTA-resistant
271 *35S::GFP* line [referred as Col(B) in the text], except for germination and early development
272 assays. Triple *snrk2.2/snrk2.3/snrk1α1-3* mutants (referred as *snrk2d*/*α1* in the text) were
273 obtained by crossing *snrk1α1-3* to the *snrk2.2/snrk2.3* double mutant (*snrk2d*) [7].
274
275 **Phenotype Assays**
276 For assays of ABA sensitivity during germination and early seedling development, seeds were
277 plated on 0.5X MS supplemented or not with ABA, and radicle emergence and cotyledon
278 greening were computed over time under a stereoscope.
279 For assaying ABA sensitivity during root development, seedlings were grown vertically for 6
280 days in 0.5X MS (supplied with BASTA in experiments with the *sesquiα2* mutant) and
281 transferred to 0.5X MS plates supplemented or not with ABA for 8 more days. All computed
282 parameters relate to the region of the root that developed after transferring the seedlings to new
283 mock or ABA plates. For LRs only those ≥ 0.5 mm long were considered.
284
285 **Co-immunoprecipitation experiments**
286 <u>*Interaction of SnRKs with TOR and RAPTOR*</u>
287 For assessing the interaction of SnRKs with TOR and RAPTOR, seedlings
288 (*proSnRK1α1::SnRK1α1-GFP*, *proSnRK2.2::SnRK2.2-GFP* and *35S::GFP*) were grown on
289 0.5X MS + 0.5% sucrose for 14d (7d in solid medium and 7d in liquid culture) and treated with
290 50 µM ABA for 40 min. GFP-tagged proteins were immunoprecipitated from whole seedling
291 cleared protein extracts using super-paramagnetic µMAC beads coupled to monoclonal anti-
292 GFP antibody (Miltenyi Biotec), and co-immunoprecipitated proteins were analyzed by
293 Western blotting using anti-GFP, anti-TOR, anti-RAPTOR, anti-SnRK1α1 and anti-SnRK2
294 antibodies.

295 For immunoprecipitation of endogenous TOR, the anti-TOR antibody was coupled to
296 Dynabeads™ Protein A (Invitrogen™) prior to its addition to the whole seedling cleared protein
297 extracts. Co-immunoprecipitated proteins were analyzed by Western blot with anti-TOR, anti-
298 SnRK1α1 and anti-SnRK2s antibodies.
299
300 *Interaction of SnRK1 with SnRK2 and PP2CA*
301 For assessing the interaction of SnRK1 with SnRK2 and PP2CA, seedlings
302 (*proSnRK1α1::SnRK1α1-GFP*, *proSnRK2.2::SnRK2.2-GFP* and *35S::GFP*) were grown on
303 0.5X MS + 0.5% sucrose for 14d (7d in solid medium and 7d in liquid culture), and roots were
304 rapidly harvested following a 3h treatment with 50 µM ABA. GFP-tagged proteins were
305 immunoprecipitated from cleared protein extracts using super-paramagnetic µMAC beads
306 coupled to monoclonal anti-GFP antibody (Miltenyi Biotec), and co-immunoprecipitated
307 proteins were analyzed by Western blotting using anti-GFP, anti-SnRK1α1, anti-SnRK2, and
308 anti-PP2CA[30] antibodies. When indicated, the SnRK1-SnRK2 interaction was analyzed also
309 from whole seedlings following a 40 min treatment with 50 µM ABA as explained above for
310 the interaction with TOR.
311
312 **RPS6^{S240} phosphorylation assays**
313 Seedlings were grown on 0.5X MS + 0.5% sucrose for 12 d (6 d in solid medium ± BASTA
314 and 6d in liquid culture) and treated with mock, 50 µM ABA, 10 µM torin2 or 2 µM AZD8055
315 during 4 h. For the ABA time course, ABA (50 µM) was added 1 h after the onset of the lights
316 and samples were collected immediately (T0) or after 15, 30, 45, 60 and 240 min. For the
317 nutrient supplementation time course, the growth medium (0.5X MS + 0.5% sucrose) was
318 replaced with fresh medium 1 h after the onset of the lights and seedlings were immediately
319 collected (T0) or after 30, 60 and 180 min. For the sudden darkness experiments, samples were
320 collected 3h after the onset of the lights (T0) or after 1 or 3 h of incubation in the dark. Samples
321 were analyzed by Western Blot with anti-phospho-RPS6^{S240} and anti-RPS6 antibodies.
322
323 **Custom-made SnRK1α1 and SnRK1α2 antibodies**
324 Polyclonal *Arabidopsis* SnRK1α1 and SnRK1α2 antibodies were obtained by conjugating
325 synthetic peptides (CTMEGTPRMHPAESVA and CTTDSGSNPMRTPEAGA, respectively;
326 produced by Cocalico Biologicals, Inc. USA) to keyhole limpet hemocyanin and injecting two
327 rabbits (performed by Cocalico Biologicals). Antibodies were affinity-purified using the

328 original peptides linked to a SulfoLink matrix (Pierce) following instructions by the
329 manufacturer.
330

331 **Data availability**

332 All data supporting the findings of this study are available in the main text or the Supplementary
333 Information. Additional data related to this study are available from the corresponding author
334 upon request. All biological materials used in this study are available from the corresponding
335 author on reasonable request.

336

337 **References**

338 1 Huot, B., Yao, J., Montgomery, B. L. & He, S. Y. Growth-defense tradeoffs in plants: a
339 balancing act to optimize fitness. *Mol Plant* **7**, 1267-1287, (2014).
340 2 Baena-Gonzalez, E., Rolland, F., Thevelein, J. M. & Sheen, J. A central integrator of
341 transcription networks in plant stress and energy signalling. *Nature* **448**, 938-942, (2007).
342 3 Baena-Gonzalez, E. & Sheen, J. Convergent energy and stress signaling. *Trends Plant Sci* **13**,
343 474-482, (2008).
344 4 Nukarinen, E. *et al.* Quantitative phosphoproteomics reveals the role of the AMPK plant
345 ortholog SnRK1 as a metabolic master regulator under energy deprivation. *Sci Rep* **6**, 31697,
346 (2016).
347 5 Rodrigues, A. *et al.* ABI1 and PP2CA phosphatases are negative regulators of Snf1-related
348 protein kinase1 signaling in Arabidopsis. *Plant Cell* **25**, 3871-3884, (2013).
349 6 Nakashima, K., Yamaguchi-Shinozaki, K. & Shinozaki, K. The transcriptional regulatory
350 network in the drought response and its crosstalk in abiotic stress responses including
351 drought, cold, and heat. *Front Plant Sci* **5**, 170, (2014).
352 7 Fujii, H., Verslues, P. E. & Zhu, J. K. Identification of two protein kinases required for abscisic
353 acid regulation of seed germination, root growth, and gene expression in Arabidopsis. *Plant*
354 *Cell* **19**, 485-494, (2007).
355 8 Mustilli, A. C., Merlot, S., Vavasseur, A., Fenzi, F. & Giraudat, J. Arabidopsis OST1 protein
356 kinase mediates the regulation of stomatal aperture by abscisic acid and acts upstream of
357 reactive oxygen species production. *Plant Cell* **14**, 3089-3099, (2002).
358 9 Umezawa, T. *et al.* Type 2C protein phosphatases directly regulate abscisic acid-activated
359 protein kinases in Arabidopsis. *Proc Natl Acad Sci U S A* **106**, 17588-17593, (2009).
360 10 Vlad, F. *et al.* Protein phosphatases 2C regulate the activation of the Snf1-related kinase
361 OST1 by abscisic acid in Arabidopsis. *Plant Cell* **21**, 3170-3184, (2009).
362 11 Yoshida, R. *et al.* The regulatory domain of SRK2E/OST1/SnRK2.6 interacts with ABI1 and
363 integrates abscisic acid (ABA) and osmotic stress signals controlling stomatal closure in
364 Arabidopsis. *J Biol Chem* **281**, 5310-5318, (2006).
365 12 Ma, Y. *et al.* Regulators of PP2C phosphatase activity function as abscisic acid sensors.
366 *Science* **324**, 1064-1068, (2009).
367 13 Park, S. Y. *et al.* Abscisic acid inhibits type 2C protein phosphatases via the PYR/PYL family of
368 START proteins. *Science* **324**, 1068-1071, (2009).

14 Bitrian, M., Roodbarkelari, F., Horvath, M. & Koncz, C. BAC-recombineering for studying plant gene regulation: developmental control and cellular localization of SnRK1 kinase subunits. *Plant J* **65**, 829-842, (2011).
15 Jossier, M. *et al.* SnRK1 (SNF1-related kinase 1) has a central role in sugar and ABA signalling in Arabidopsis thaliana. *Plant J* **59**, 316-328, (2009).
16 Lin, C. R. *et al.* SnRK1A-Interacting Negative Regulators Modulate the Nutrient Starvation Signaling Sensor SnRK1 in Source-Sink Communication in Cereal Seedlings under Abiotic Stress. *Plant Cell*, (2014).
17 Lu, C. A. *et al.* The SnRK1A protein kinase plays a key role in sugar signaling during germination and seedling growth of rice. *Plant Cell* **19**, 2484-2499, (2007).
18 Radchuk, R. *et al.* Sucrose non-fermenting kinase 1 (SnRK1) coordinates metabolic and hormonal signals during pea cotyledon growth and differentiation. *Plant J* **61**, 324-338, (2010).
19 Radchuk, R., Radchuk, V., Weschke, W., Borisjuk, L. & Weber, H. Repressing the expression of the SUCROSE NONFERMENTING-1-RELATED PROTEIN KINASE gene in pea embryo causes pleiotropic defects of maturation similar to an abscisic acid-insensitive phenotype. *Plant Physiol* **140**, 263-278, (2006).
20 Tsai, A. Y. & Gazzarrini, S. AKIN10 and FUSCA3 interact to control lateral organ development and phase transitions in Arabidopsis. *Plant J* **69**, 809-821, (2012).
21 Tsai, A. Y. & Gazzarrini, S. Trehalose-6-phosphate and SnRK1 kinases in plant development and signaling: the emerging picture. *Front Plant Sci* **5**, 119, (2014).
22 Zhang, Y. *et al.* Arabidopsis sucrose non-fermenting-1-related protein kinase-1 and calcium-dependent protein kinase phosphorylate conserved target sites in ABA response element binding proteins. *Ann Appl Biol* **153**, 401-409, (2008).
23 Ramon, M. *et al.* Default Activation and Nuclear Translocation of the Plant Cellular Energy Sensor SnRK1 Regulate Metabolic Stress Responses and Development. *Plant Cell* **31**, 1614-1632, (2019).
24 Lopez-Molina, L., Mongrand, S. & Chua, N. H. A postgermination developmental arrest checkpoint is mediated by abscisic acid and requires the ABI5 transcription factor in Arabidopsis. *Proc Natl Acad Sci U S A* **98**, 4782-4787, (2001).
25 Garcia, D. & Shaw, R. J. AMPK: Mechanisms of Cellular Energy Sensing and Restoration of Metabolic Balance. *Mol Cell* **66**, 789-800, (2017).
26 Dobrenel, T. *et al.* The Arabidopsis TOR Kinase Specifically Regulates the Expression of Nuclear Genes Coding for Plastidic Ribosomal Proteins and the Phosphorylation of the Cytosolic Ribosomal Protein S6. *Front Plant Sci* **7**, 1611, (2016).
27 Wang, P. *et al.* Reciprocal Regulation of the TOR Kinase and ABA Receptor Balances Plant Growth and Stress Response. *Mol Cell* **69**, 100-112 e106, (2018).
28 Van Leene, J. *et al.* Capturing the phosphorylation and protein interaction landscape of the plant TOR kinase. *Nat Plants* **5**, 316-327, (2019).
29 Dietrich, D. *et al.* Root hydrotropism is controlled via a cortex-specific growth mechanism. *Nat Plants* **3**, 17057, (2017).
30 Wu, Q. *et al.* Ubiquitin Ligases RGLG1 and RGLG5 Regulate Abscisic Acid Signaling by Controlling the Turnover of Phosphatase PP2CA. *Plant Cell* **28**, 2178-2196, (2016).
31 Belin, C. *et al.* Identification of features regulating OST1 kinase activity and OST1 function in guard cells. *Plant Physiol* **141**, 1316-1327, (2006).
32 Fujii, H. & Zhu, J. K. Arabidopsis mutant deficient in 3 abscisic acid-activated protein kinases reveals critical roles in growth, reproduction, and stress. *Proc Natl Acad Sci USA* **106**, 8380-8385, (2009).
33 Fujita, Y. *et al.* Three SnRK2 protein kinases are the main positive regulators of abscisic acid signaling in response to water stress in Arabidopsis. *Plant Cell Physiol* **50**, 2123-2132, (2009).

419 34 Nakashima, K. *et al.* Three Arabidopsis SnRK2 protein kinases, SRK2D/SnRK2.2,
420 SRK2E/SnRK2.6/OST1 and SRK2I/SnRK2.3, involved in ABA signaling are essential for the
421 control of seed development and dormancy. *Plant Cell Physiol* **50**, 1345-1363, (2009).
422 35 Fujii, H. *et al.* In vitro reconstitution of an abscisic acid signalling pathway. *Nature* **462**, 660-
423 664, (2009).
424 36 Shen, W., Reyes, M. I. & Hanley-Bowdoin, L. Arabidopsis protein kinases GRIK1 and GRIK2
425 specifically activate SnRK1 by phosphorylating its activation loop. *Plant Physiol* **150**, 996-
426 1005, (2009).
427 37 Cheng, C. *et al.* SCFAtPP2-B11 modulates ABA signaling by facilitating SnRK2.3 degradation in
428 Arabidopsis thaliana. *PLoS Genet* **13**, e1006947, (2017).
429 38 Harthill, J. E. *et al.* Phosphorylation and 14-3-3 binding of Arabidopsis trehalose-phosphate
430 synthase 5 in response to 2-deoxyglucose. *Plant J* **47**, 211-223, (2006).
431 39 Song, Y. *et al.* Identification of novel interactors and potential phosphorylation substrates of
432 GsSnRK1 from wild soybean (Glycine soja). *Plant Cell Environ*, (2018).
433 40 Wang, X., Du, Y. & Yu, D. Trehalose phosphate synthase 5-dependent trehalose metabolism
434 modulates basal defense responses in Arabidopsis thaliana. *J Integr Plant Biol* **61**, 509-527,
435 (2019).
436 41 Broeckx, T., Hulsmans, S. & Rolland, F. The plant energy sensor: evolutionary conservation
437 and divergence of SnRK1 structure, regulation, and function. *J Exp Bot* **67**, 6215-6252, (2016).
438 42 Wang, Y. *et al.* AKINbeta1, a subunit of SnRK1, regulates organic acid metabolism and acts as
439 a global modulator of genes involved in carbon, lipid, and nitrogen metabolism. *J Exp Bot* **71**,
440 1010-1028, (2020).
441 43 Yoshida, T. *et al.* The Role of Abscisic Acid Signaling in Maintaining the Metabolic Balance
442 Required for Arabidopsis Growth under Nonstress Conditions. *Plant Cell* **31**, 84-105, (2019).
443 44 Zheng, Z. *et al.* The protein kinase SnRK2.6 mediates the regulation of sucrose metabolism
444 and plant growth in Arabidopsis. *Plant Physiol* **153**, 99-113, (2010).
445 45 Cutler, S. R., Rodriguez, P. L., Finkelstein, R. R. & Abrams, S. R. Abscisic acid: emergence of a
446 core signaling network. *Annu Rev Plant Biol* **61**, 651-679, (2010).
447 46 Kravchenko, A. *et al.* Mutations in the Arabidopsis Lst8 and Raptor genes encoding partners
448 of the TOR complex, or inhibition of TOR activity decrease abscisic acid (ABA) synthesis.
449 *Biochem Biophys Res Commun* **467**, 992-997, (2015).
450 47 Salem, M. A., Li, Y., Wiszniewski, A. & Giavalisco, P. Regulatory-associated protein of TOR
451 (RAPTOR) alters the hormonal and metabolic composition of Arabidopsis seeds, controlling
452 seed morphology, viability and germination potential. *Plant J* **92**, 525-545, (2017).
453 48 Bakshi, A. *et al.* Ectopic expression of Arabidopsis Target of Rapamycin (AtTOR) improves
454 water-use efficiency and yield potential in rice. *Sci Rep* **7**, 42835, (2017).
455 49 De Smet, I. *et al.* An abscisic acid-sensitive checkpoint in lateral root development of
456 Arabidopsis. *Plant J* **33**, 543-555, (2003).
457 50 Hrabak, E. M. *et al.* The Arabidopsis CDPK-SnRK superfamily of protein kinases. *Plant Physiol*
458 **132**, 666-680, (2003).
459 51 Hauser, F., Waadt, R. & Schroeder, J. I. Evolution of abscisic acid synthesis and signaling
460 mechanisms. *Curr Biol* **21**, R346-355, (2011).
461 52 Umezawa, T. *et al.* Molecular basis of the core regulatory network in ABA responses: sensing,
462 signaling and transport. *Plant Cell Physiol* **51**, 1821-1839, (2010).

463

464

465

466 **FIGURE LEGENDS**

467 **Fig. 1. SnRK1 *sesquiα2* mutants show defective growth repression in ABA. a,** SnRK1
468 *sesquiα2-1* and *sesquiα2-2* mutants have higher cotyledon greening rates than control plants in
469 ABA. Graph shows the percentage of green and expanded cotyledons in seedlings grown for
470 15d on 0.5X MS with or without ABA (n=3, 100 seeds per genotype each experiment; error
471 bars, SEM). *p*-values denote statistically significant differences for comparisons to the Col-0
472 control (one-way ANOVA with Tukey HSD test). **b,** SnRK1 *sesquiα2-1* and *sesquiα2-2*
473 mutants have higher lateral root (LR) density than control plants in ABA. Left panels,
474 representative pictures of seedlings grown vertically on 0.5X MS medium with BASTA for 5d
475 and transferred to 0.5X MS with or without ABA for 8d. Right panels, quantification of primary
476 root (PR) length and LR density from 6 independent experiments (total number of plates: WT
477 mock n=16, *sesquiα2-1* mock n=7, *sesquiα2-2* mock n=9, WT ABA n=24, *sesquiα2-1* ABA
478 n=12, *sesquiα2-2* mock n=12; total number of seedlings: 36-72 per genotype and condition).
479 Upper and lower box boundaries represent the first and third quantiles, respectively, horizontal
480 lines mark the median and whiskers mark the highest and lowest values. *p*-values denote
481 statistically significant differences for comparisons to control plants (one-way ANOVA with
482 Tukey HSD test). Col(B), BASTA-resistant Col-0 expressing *35S::GFP*, used as control. **c,**
483 Repression of TOR signaling in response to ABA is slower in SnRK1 *sesquiα2-1* mutants than
484 in Col(B) control plants. Seedlings were treated with 50 µM ABA for the indicated times and
485 TOR activity was subsequently analyzed from total protein extracts using immunoblotting and
486 $RPS6^{S240}$ phosphorylation as readout. Graph corresponds to the average of 5 independent
487 experiments (error bars, SEM). *p*-values denote statistically significant differences (two-tailed
488 Welch t-test). All samples were run in the same gel but images were cropped for showing first
489 the Col(B) series. **d,** TOR interacts with SnRK1α1 and the interaction is enhanced two-fold in
490 ABA. 14d-old seedlings expressing SnRK1α1-GFP, were treated with mock or 50 µM ABA
491 for 40 min, GFP-tagged proteins were immunoprecipitated from total protein extracts and co-
492 immunoprecipitation of TOR was assessed by immunodetection with TOR specific antibodies.
493 Two independent experiments are shown. Numbers refer to the relative intensity of the
494 corresponding TOR band. **e, f,** TOR is not co-immunoprecipitated with GFP alone (**e**) or with
495 SnRK2.2-GFP (**f**). 14d-old seedlings expressing *35S::GFP* or *proSnRK2.2::SnRK2.2-GFP*
496 were treated and analyzed as in (**d**)**.** Two independent experiments were performed with similar
497 results (**e**, **f**).

498

499 **Fig. 2. SnRK2s interact with SnRK1 in a PP2CA-dependent manner. a, b,** SnRK1α1 and
500 SnRK2.2 interact *in planta* and the interaction is reduced over 2-fold in ABA. Seedlings
501 expressing *proSnRK1α1:SnRK1α1-GFP* (**a**) or *proSnRK2.2:SnRK2.2-GFP* (**b**) were mock- or
502 ABA-treated, GFP-tagged proteins were immunoprecipitated from roots and co-
503 immunoprecipitation of SnRK2 and SnRK1α1, respectively was assessed by immunodetection
504 with the indicated antibodies. Graphs correspond to the average of 4 independent experiments
505 (error bars, SEM). *p*-values denote statistically significant differences (**a**, two-tailed Student t-
506 test, **b**, two-tailed Welch t-test). **c, d,** PP2CA co-immunoprecipitates with SnRK1α1-GFP (**c**)
507 and SnRK2.2-GFP (**d**) and, proportionally to the total PP2CA levels, both interactions are
508 reduced in ABA. Seedlings expressing *proSnRK1α1::SnRK1α1-GFP* or
509 *proSnRK2.2::SnRK2.2-GFP* were mock- or ABA-treated, GFP-tagged proteins were
510 immunoprecipitated from roots and co-purifying proteins were analyzed by immunoblotting
511 with specific antibodies. Two independent experiments were performed with similar results (**c**,
512 **d**). **e,** BiFC experiments show that SnRK1α1 and SnRK2.2 interact only in the presence of
513 PP2CA and this interaction occurs mostly in the nucleus. Left panels, representative pictures of
514 *Nicotiana benthamiana* epidermal cells expressing YFP^N-SnRK1α1 and YFP^C-SnRK2.2 with
515 a nuclear localized RFP (mRFP-NLS) or with PP2CA-RFP. Right panels, quantification of RFP
516 and YFP signals (error bars, SEM; mRFP-NLS samples, n=9; PP2CA-RFP samples, n=14).
517 Scale bars, 30 µm. Two independent experiments were performed with similar results.

518

519 **Fig. 3. SnRK2s regulate TOR and growth *via* SnRK1. a,** The *snrk1α1-3* mutation increases
520 the ABA insensitivity of the *snrk2d* mutant during germination. Upper two panels, seeds of
521 Col-0, *snrk2d*, and *snrk2d snrk1α1* (*snrk2d/1α1*) mutants were plated on 0.5X MS with or
522 without ABA and radicle emergence was scored at the indicated times (shown are percentages
523 in ABA as compared to the mock condition; n=3, 50 seeds per genotype each experiment; error
524 bars, SEM). Different letters indicate statistically significant differences for each time point
525 ($p<0.05$, one-way ANOVA with Tukey HSD test). Lower panel, degree of ABA insensitivity
526 computed by normalizing the parameters scored in ABA to the corresponding mock control
527 (error bars, SEM). *p*-values refer to the differences between *snrk2d/1α1* and *snrk2d* (one-way
528 ANOVA with Tukey HSD test for each time point). **b,** The *snrk1α1-3* mutation increases the
529 cotyledon greening rates of the *snrk2d* mutant in ABA. Seeds were plated as in (**a**) and
530 cotyledon greening was scored after 16d. Graph corresponds to the average of 3 independent
531 experiments (100 seeds per genotype each experiment; error bars, SEM). *p*-values denote

532 statistically significant differences (two-tailed Student t-test). **c,** In control conditions the *snrk2d*
533 mutant has defects in primary (PR) and lateral root (LR) growth that are fully rescued by the
534 *snrk1α1* mutation. In ABA the *snrk1α1* mutation enhances the ABA hyposensitivity of the
535 *snrk2d* mutant with regard to PR length and LR density. Upper panel, representative picture of
536 seedlings grown vertically on 0.5X MS medium for 5d and transferred to 0.5X MS with or
537 without ABA for 8d. Middle panels, quantification of PR length and LR density from 3
538 independent experiments (total number of plates: WT mock n=21, *snrk2d* mock n=19,
539 *snrk2d/1α1* mock n=21, WT ABA n=21, *snrk2d* ABA n=21, *snrk2d/1α1* ABA n=21; total
540 number of seedlings: 37-42 seedlings per genotype and condition). Upper and lower box
541 boundaries represent the first and third quantiles, respectively, horizontal lines mark the median
542 and whiskers mark the highest and lowest values. Lower panels, degree of ABA insensitivity
543 computed by normalizing the parameters scored in ABA to the corresponding mock control
544 (error bars, SEM). Different letters indicate statistically significant differences ($p<0.05$, one-
545 way ANOVA with Tukey HSD test). **d,** The *snrk2d* mutant exhibits hyposensitivity to TOR
546 inhibition by AZD8055 and this is fully rescued by the *snrk1α1* mutation. Left panel,
547 representative pictures of seedlings grown vertically on 0.5X MS medium for 7d and transferred
548 to 0.5X MS with or without the indicated AZD concentrations for 7d. Percentage values refer
549 to the average increment in PR length (from the point of transfer) of the *snrk2d* as compared to
550 that of the WT in each condition. Right panel, quantification of primary root (PR) length from
551 2 independent experiments (total number of plates per genotype: mock, n=12; 0.2 μM AZD,
552 n=11, 0.5 μM AZD, n=10; total number of seedlings: 20-24 per genotype and condition; error
553 bars, SEM). Different letters indicate statistically significant differences ($p<0.0001$, two-way
554 ANOVA with Tukey´s HSD test). **e,** The *snrk2d* mutant shows defective induction of TOR
555 signaling and this is fully rescued by the *snrk1α1* mutation. Samples were collected at the
556 indicated times following replacement of the growth medium with fresh medium (FM). TOR
557 activity was analyzed from total protein extracts using immunoblotting and $RPS6^{S240}$
558 phosphorylation as readout. Graph corresponds to the average of 5 independent experiments
559 (error bars, SEM). Different letters indicate statistically significant differences for each time
560 point ($p<0.05$, one-way ANOVA with Tukey HSD test). **f,** The *snrk2d* mutant shows higher
561 phosphorylation of TPS5, indicating higher SnRK1 activity. WT and *snrk2d* seedlings were
562 grown as in panel (**c**) (only mock conditions). Whole seedlings were harvested and total protein
563 extracts were analyzed using Phos-tag gels to separate TPS5 phospho-proteoforms from the
564 non-phosphorylated protein, followed by immunoblotting with a TPS5 antibody (lower panel).
565 Extracts from the *tps5-1* mutant were included in regular Western blot analyses (upper pannel)

566 as control for the specificity of the TPS5 antibody. All samples were run in the same gel but
567 images were cropped for showing *tps5-1* alongside WT and *snrk2d*. Graph corresponds to the
568 average of 3 independent experiments (error bars, SEM). **g,** The interaction between SnRK1α1
569 and the SnRK1β1 regulatory subunit is enhanced in the *snrk2d* mutant. SnRK1α1 was
570 immunoprecipitated from total protein extracts of 14d-old WT and *snrk2d* seedlings and co-
571 purifying proteins were analyzed by immunoblotting with a SnRK1β1 antibody. Graph
572 corresponds to the average of 3 independent experiments (error bars, SEM). *p*-values denote
573 statistically significant differences (**f**, two-tailed ratio t-test; **g**, two-tailed Student t-test).

574

575 **Fig. 4. A dual function of SnRK2 kinases in the regulation of SnRK1 and growth.** Upper
576 panel: under optimal conditions, SnRK2s promote growth. In the absence of ABA, SnRK2s are
577 required for the formation of SnRK1 repressor complexes that harbor also PP2Cs. Sequestration
578 of SnRK1 in these complexes is important to prevent its interaction with TOR and thereby to
579 allow growth when conditions are favorable. Lower panel: under stress conditions, SnRK2s
580 inhibit growth. In the presence of ABA, SnRK2 and PP2C-containing SnRK1 repressor
581 complexes disassemble through canonical ABA signaling involving the sequestration of PP2Cs
582 by the ABA-bound PYR/PYL receptors. Disassembly of the complexes releases SnRK2s and
583 SnRK1α to trigger stress responses and inhibit growth. This is partly accomplished by direct
584 TOR repression by SnRK1 but may also involve co-participation of SnRK2 kinases. Inactive
585 components are shown in white. Dark blue and dark orange denote components that are active
586 under optimal conditions or under stress, respectively.

587

588 **Acknowledgements**

589 The authors would like to thank J-K. Zhu for the *snrk2* mutants, M. Bennett for the SnRK2.2-
590 GFP line, C. Koncz for the SnRK1-GFP line, X. Li for the SnRK2.3-FLAG OE line, J.
591 Schroeder for the GFP-His-FLAG and SnRK2.6-His-FLAG OE lines, C. Mackintosh for the
592 TPS5 antibody, and the Nottingham Arabidopsis stock center (NASC) for T-DNA mutant
593 seeds. The IGC Plant Facility (Vera Nunes) is thanked for excellent plant care. This work was
594 supported by Fundação para a Ciência e a Tecnologia through the R&D Units
595 UIDB/04551/2020 (GREEN-IT - Bioresources for Sustainability) and UID/MAR/04292/2019,
596 FCT projects PTDC/BIA-PLA/7143/2014, LISBOA-01-0145-FEDER-028128, and

PTDC/BIA-BID/32347/2017, and FCT fellowships/contracts SFRH/BD/122736/2016 (MA), SFRH/BPD/109336/2015 (AC), PD/BD/150239/2019 (DRB), and IF/00804/2013 (EBG). Work in Dr Rodriguez's lab was funded by MCIU grant BIO2017-82503-R. CM thanks the LabEx Paris Saclay Plant Sciences-SPS (ANR-10-LABX-040-SPS) for support. BBP was funded by Programa VALi+d GVA APOSTD/2017/039. This project has received funding from the European Union Horizon 2020 research and innovation programme (Grant Agreement number: 867426 —ABA-GrowthBalance — H2020-WF-2018-2020/H2020-WF-01-2018, awarded to BBP).

This work is dedicated to the memory of our beloved friend and colleague Américo Rodrigues.

Author contributions

BBP, MA, and CV designed and performed experiments, and analyzed and interpreted data. LF performed and analyzed the root phenotyping experiments in low light and AZD. AC generated and characterized molecularly the *sesquiα2* mutant lines and provided strong conceptual support. DRB performed protein immunoprecipitation from protoplasts and *in vitro* kinase assays. AR contributed to the general conception of the project and the initial exploratory experiments. CM contributed the phospho-RPS6 antibody and expertise on molecular and plant phenotype assays related to TOR activity. PLR contributed tools and expertise on PP2C-SnRK2 interactions and ABA signaling, and actively supported the conceptual work. BBP and EBG prepared the figures and wrote the manuscript. EBG conceived the project and directed and supervised all of the research. All authors read and approved the manuscript.

Competing interests

The authors declare no competing interests.

Figure 1

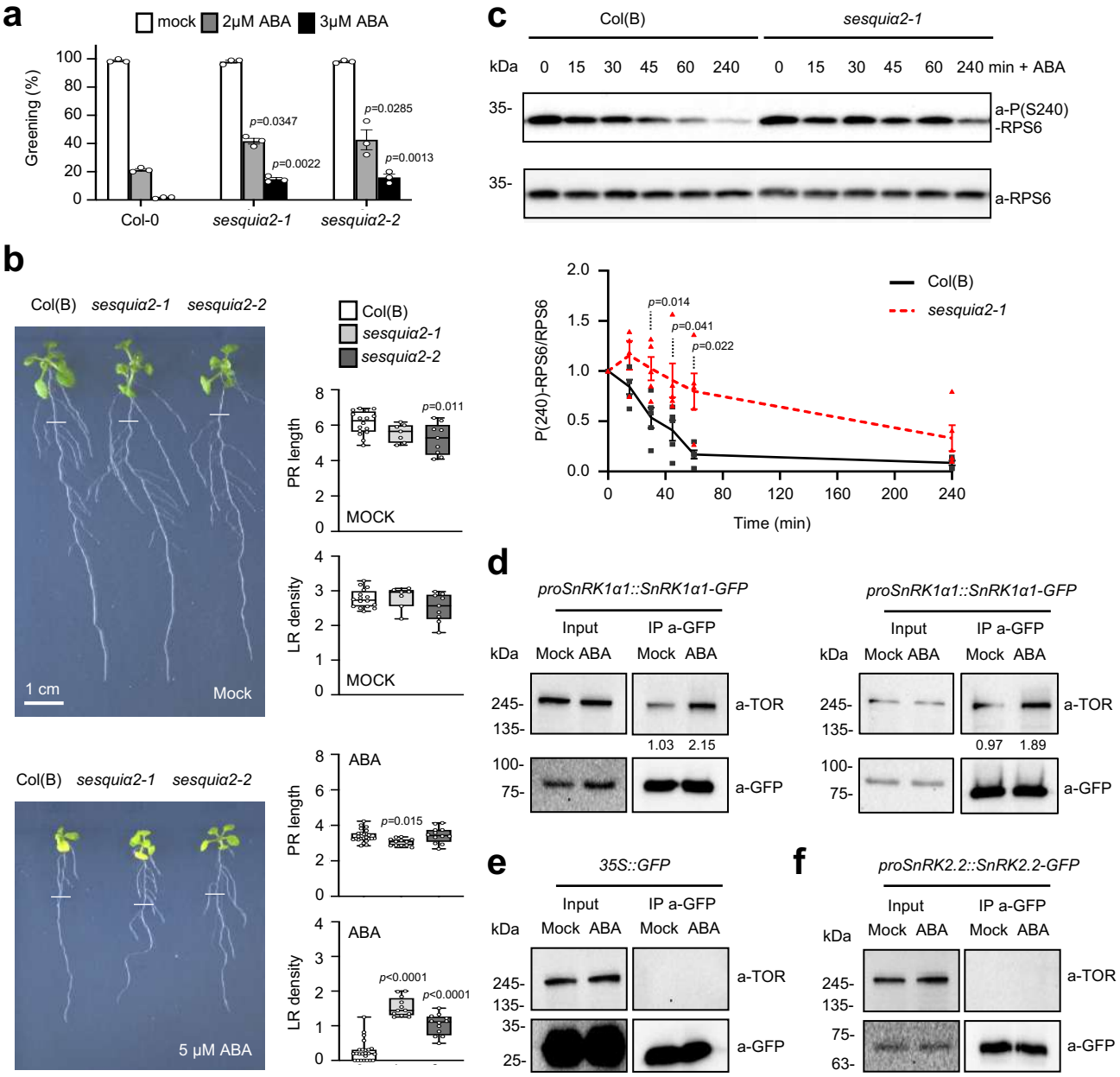
a
mock
2μM ABA
3μM ABA
Greening (%)
100
80
60
40
20
0
p=0.0347
p=0.0022
p=0.0285
p=0.0013
Col-0
sesquia2-1
sesquia2-2
b
Col(B)
sesquia2-1
sesquia2-2
1 cm
Mock
PR length
LR density
MOCK
p=0.011
ABA
p=0.015
p<0.0001
p<0.0001
5 μM ABA
c
Col(B)
sesquia2-1
kDa
0 15 30 45 60 240 0 15 30 45 60 240 min + ABA
35-
a-P(S240)
-RPS6
a-RPS6
P(240)-RPS6/RPS6
Time (min)
p=0.014
p=0.041
p=0.022
d
proSnRK1α1::SnRK1α1-GFP
Input
IP a-GFP
Mock ABA Mock ABA
245-
135-
100-
75-
a-TOR
a-GFP
1.03 2.15
0.97 1.89
e
35S::GFP
35-
25-
f
proSnRK2.2::SnRK2.2-GFP
63-

Figure 2

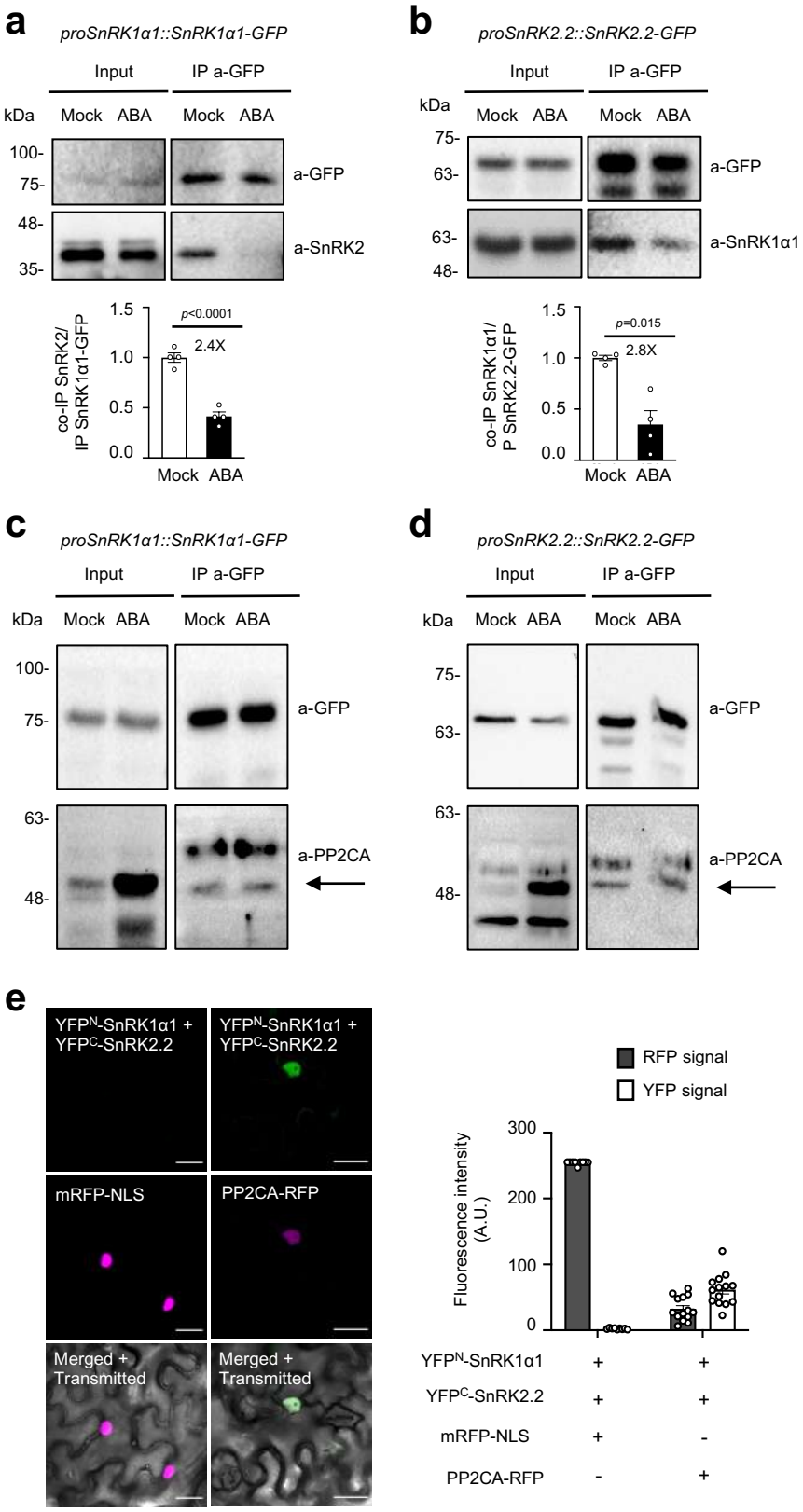
a
proSnRK1α1::SnRK1α1-GFP
Input
IP a-GFP
kDa
Mock ABA Mock ABA
100-
75-
48-
35-
a-GFP
a-SnRK2
co-IP SnRK2/ IP SnRK1α1-GFP
1.5
1.0
0.5
0.0
p<0.0001
2.4X
Mock ABA
b
proSnRK2.2::SnRK2.2-GFP
Input
IP a-GFP
kDa
Mock ABA Mock ABA
75-
63-
63-
48-
a-GFP
a-SnRK1α1
co-IP SnRK1α1/ P SnRK2.2-GFP
1.5
1.0
0.5
0.0
p=0.015
2.8X
Mock ABA
c
proSnRK1α1::SnRK1α1-GFP
Input
IP a-GFP
kDa
Mock ABA Mock ABA
100-
75-
63-
48-
a-GFP
a-PP2CA
d
proSnRK2.2::SnRK2.2-GFP
Input
IP a-GFP
kDa
Mock ABA Mock ABA
75-
63-
63-
48-
a-GFP
a-PP2CA
e
YFPN-SnRK1α1 + YFPC-SnRK2.2
YFPN-SnRK1α1 + YFPC-SnRK2.2
mRFP-NLS
PP2CA-RFP
Merged + Transmitted
Merged + Transmitted
RFP signal
YFP signal
Fluorescence intensity (A.U.)
300
200
100
0
YFPN-SnRK1α1 + +
YFPC-SnRK2.2 + +
mRFP-NLS + -
PP2CA-RFP - +

Figure 3

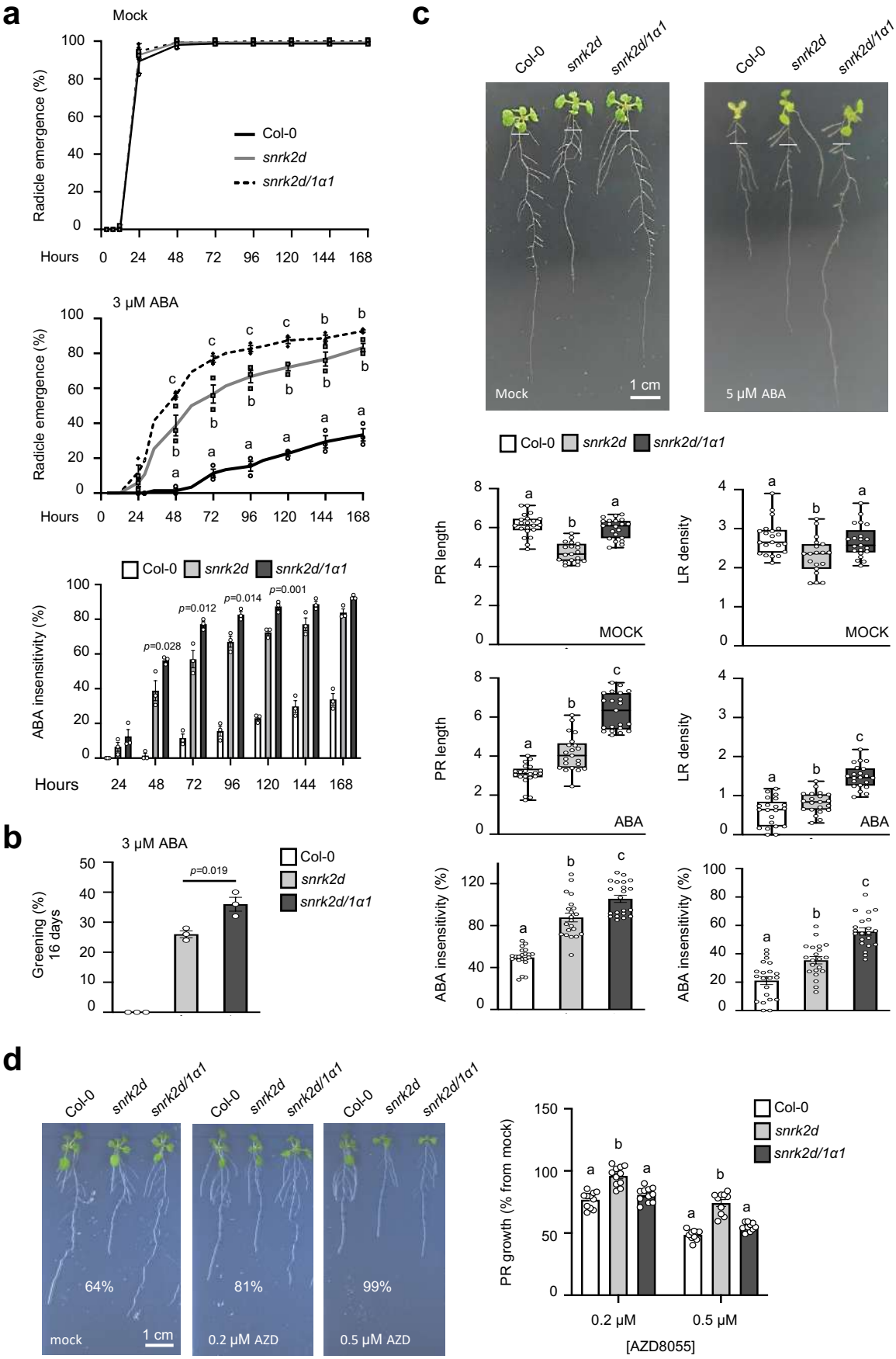
a
Mock
Radicle emergence (%)
Col-0
snrk2d
snrk2d/1α1
Hours
3 μM ABA
ABA insensitivity (%)
p=0.028
p=0.012
p=0.014
p=0.001
b
3 μM ABA
Greening (%) 16 days
p=0.019
c
Col-0
snrk2d
snrk2d/1α1
Mock
1 cm
5 μM ABA
PR length
LR density
MOCK
ABA
ABA insensitivity (%)
d
64%
81%
99%
mock
0.2 μM AZD
0.5 μM AZD
PR growth (% from mock)
0.2 μM
0.5 μM
[AZD8055]

Figure 3 (cont.)

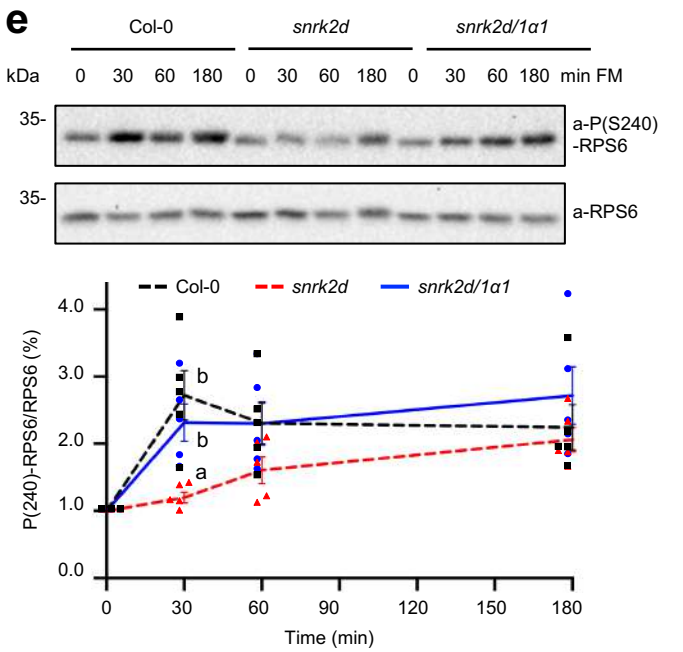

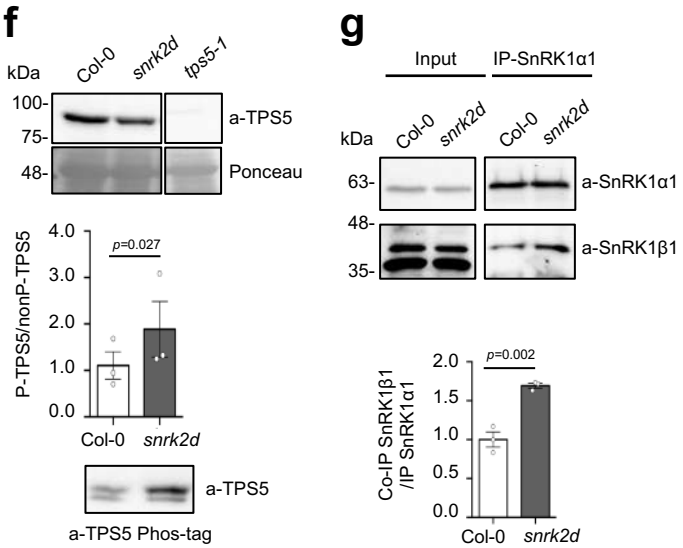

Figure 4

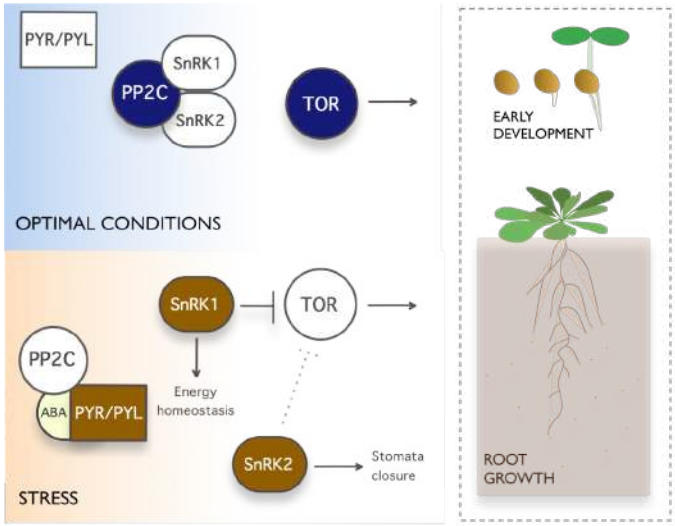
PYR/PYL
SnRK1
PP2C
SnRK2
TOR
OPTIMAL CONDITIONS
SnRK1
TOR
PP2C
ABA
PYR/PYL
Energy homeostasis
SnRK2
Stomata closure
STRESS
EARLY DEVELOPMENT
ROOT GROWTH

SUPPLEMENTARY FIGURE LEGENDS

Supplementary Fig. 1. Generation of SnRK1 *sesquiα2* mutants. a, Scheme showing the insertion sites of the *snrk1α1* and *snrk1α2* T-DNA mutants used in this study. **b,** Confirmation of *sesquiα2* mutant identity by genotyping. Lanes containing samples from *sesquiα2-1* and *sesquiα2-2* mutants (lanes 4 and 6, respectively) are marked in red. At least 3 independent analyses were performed with similar results. **c,** Accumulation of SnRK1α1 and SnRK1α2 proteins is defective in the *sesquiα2* mutants. Left panels, representative blots showing the accumulation of SnRK1α1 and SnRK1α2 in the indicated genotypes. SnRK1α T-loop phosphorylation is detected with a phospho-AMPK antibody (P-AMPK). Ponceau staining of membranes shows equal protein loading in all samples. Right panel, quantification of indicated proteins from 2 independent experiments (each with 1-4 technical replicates; error bars, SEM). Numbers refer to the genotypes shown on the right panel. *p*-values denote statistically significant differences (one-way ANOVA with Tukey HSD test). **d,** Specificity of the SnRK1α antibodies described in this study. Protoplasts were transfected with control DNA (no protein expression) or with plasmids for overexpressing HA-tagged SnRK1α1 or SnRK1α2. Immunoblots show that anti-SnRK1α1 antibodies recognize SnRK1α1 but not SnRK1α2. Conversely, anti-SnRK1α2 antibodies recognize SnRK1α2 but not SnRK1α1. Both antibodies are able to detect the corresponding endogenous proteins[1], of slightly lower molecular size. Two independent experiments were performed with similar results.

Supplementary Fig. 2. SnRK1 *sesquiα2* mutants show defective SnRK1 signaling. BASTA-selected *sesquiα2-1* and *sesquiα2-2* plants were grown on soil for 4 weeks under a 12:12h phototoperiod. Rosette leaves were detached and incubated on sterile MilliQ water in covered Petri dishes under light (control; 100 µmol $m^{-2}s^{-1}$) or darkness (energy stress) for 6h (starting 3h after the lights are on). qPCR analyses show defective induction of the indicated SnRK1 marker genes in darkness in the *sesquiα2-1* and *sesquiα2-2* mutants compared to the WT control. Upper and lower box boundaries represent the first and third quantiles, respectively, horizontal lines mark the median and whiskers mark the highest and lowest values. Six independent experiments were performed with samples consisting of 3 leaves pooled from 3 different plants. *p*-values denote statistically significant differences (two-way ANOVA with Dunnett's multiple comparison test).

Supplementary Fig. 3. Progeny from *sesquiα2* plants that develop green cotyledons in ABA have a *sesquiα2* genotype, as exemplified by analyses of the *sesquiα2-2* mutant. The

sesquiα2-2 mutant has the *snrk1α2-2* mutation in heterozygosity, and hence its seeds are a mixed population of *sesquiα2-2* and single *snrk1α1-3* mutants (Confraria *et al*., in preparation). For assays of ABA sensitivity during early seedling development, seeds from s*esquiα2-2* plants cannot be preselected on BASTA to identify true *sesquiα2* seedlings and have to be instead plated directly on medium with or without ABA (2 µM). However, after 15d, only *sesquiα2-2* seedlings develop green cotyledons in ABA, as shown by the genotyping analyses of twenty randomly selected seedlings with green cotyledons. Genotyping PCR was for *snrk1α2-2* (see also Supplementary Fig. 1), the allele segregating in the *sesquiα2-2* plants. Analyses were performed once with seeds from two independent batches.

Supplementary Fig. 4. Single *snrk1α1 and snrk1α2* mutants have mostly normal ABA sensitivity. a, Quantification of green and expanded cotyledons of SnRK1 single mutants (*snrk1α1-3*, *snrk1α2-1, snrk1α2-2*) and Col-0 wild-type seedlings grown on 0.5X MS with or without ABA for 15d. Percentage of green and expanded cotyledons in ABA as compared to the mock condition (average from 3 independent experiments, 100 seeds per genotype each; error bars, SEM). **b,** Quantification of primary root (PR) length and LR density from 5 (Col-0/ *snrk1α1-3, snrk1α2-1*) and 2 independent experiments (Col-0/*snrk1α2-2*) shows only a mild ABA hyposensitivity in the *snrk1α1-3* mutant with regard to LR density (total number of plates: WT mock n=8, *snrk1α1* mock n=8, *snrk1α2-1* mock n=8, *snrk1α2-2* mock n=8, WT ABA n=16, *snrk1α1* ABA n=16, *snrk1α2-1* ABA n=16, *snrk1α2-2* ABA n=10; total number of seedlings: 30-65 seedlings per genotype and condition). Upper and lower box boundaries represent the first and third quantiles, respectively, horizontal lines mark the median and whiskers mark the highest and lowest values. *p*-values denote statistically significant differences (one-way ANOVA with Tukey HSD test).

Supplementary Fig. 5. Several ABA responses are normal in SnRK1 *sesquiα2* mutants. a, SnRK1 *sesquiα2* mutants show normal ABA sensitivity during germination. Seeds of the indicated genotypes were plated on 0.5X MS with or without ABA and radicle emergence was scored for the indicated times (percentage in ABA as compared to the mock condition). Shown are average values from 3 independent experiments (each with 100 seeds per genotype; error bars, SEM); ns, non-significant (one-way ANOVA with Tukey HSD test). Comparisons are with regard to control plant under the same conditions. **b,** SnRK1 *sesquiα2* mutants show normal water loss rates. The *ost1* mutant shows accelerated desiccation and

serves as a positive control. Leaves of similar age were detached from 30d-old plants of the indicated genotypes (5 leaves from 5 different plants), weighed, subjected to the drying atmosphere of a laminar flow hood, and re-weighed at the indicated times. Values are averages of the percentage of initial fresh weight (error bars, SEM). *p*-values denote statistically significant differences in comparisons to the Col-0 control (one-way ANOVA with Tukey HSD test). **c,** SnRK1 *sesquiα2* mutants show normal induction of ABA marker genes. Levels of *RAB18* and *RD29A* were measured by qPCR from 14d-old seedlings growing on 0.5X MS and mock- or ABA-treated (50 μM) for 3h (n=4, corresponding to 4 independently grown seedling sets; error bars, SEM); ns, not significant (two-tailed Student t-test).

Supplementary Fig. 6. SnRK1 *sesquiα2* mutants show defective repression of LR growth in low light conditions. a, Representative picture of seedlings grown vertically on 0.5X MS medium with BASTA for 7d under normal light (100 μmol $m^{-2}s^{-1}$) and transferred to 0.5X MS under low light (40 μmol $m^{-2}s^{-1}$) for 7d. Col(B), BASTA-resistant Col-0 control plants (*35S::GFP*). **b,** Quantification of primary root (PR) length and LR density from 3 independent experiments (error bars, SEM; total number of plates: WT normal light n=15, *sesquiα2-1* normal light n=15, WT low light n=25, *sesquiα2-1* low light n=25; total number of seedlings: 37-66 per genotype and condition). *p*-value denotes statistically significant differences (two-tailed Welch t-test). ns, not significant.

Supplementary Fig. 7. Use of RPS6^{S240} phosphorylation to monitor TOR inhibition by ABA. a, Treatment of 11d-old seedlings with 50 μM ABA, 10 μM torin2 or 2 μM AZD8055 during 3h induces a strong repression of TOR activity as evidenced by the reduced RPS6^{S240} phosphorylation levels. Two independent experiments were performed with similar results. **b,** Lack of SnRK2.2, SnRK2.3, and SnRK2.6 in the *snrk2t* mutant abrogates the repression of TOR activity by ABA. Col-0 seedlings reach nearly full TOR repression within 4h, whereas no changes in TOR activity can be observed in *snrk2t* seedlings within this timeframe. Graph corresponds to the average of 3 independent experiments (error bars, SEM). *p*-values denote statistically significant differences (two-tailed Student t-test).

Supplementary Fig. 8. RAPTOR and TOR interact with SnRK1α1. a, RAPTOR interacts with SnRK1α1 in mock and ABA. 14d-old seedlings expressing *proSnRK1α1::SnRK1α1-GFP* were treated with mock or 50 μM ABA for 40 min, GFP-tagged proteins were

immunoprecipitated from total protein extracts and co-immunoprecipitation of RAPTOR was assessed by immunodetection with RAPTOR-specific antibodies. Numbers refer to the relative intensity of the corresponding RAPTOR band. Two independent experiments are shown. RAPTOR does not co-immunoprecipitate with GFP alone **(b)** or with SnRK2.2-GFP **(c)**. Two independent experiments were performed with similar results (**b**, **c**). GFP blots in **a**, **b**, and **c**, are the same as in Figs. 1d, 1e, and 1f, respectively (same membranes used to detect TOR and RAPTOR). **d,** Reciprocal immunoprecipitation assays corroborate the SnRK1α1-TOR interaction. 14d-old seedlings were treated with mock or 50 μM ABA for 40 min, endogenous TOR was immunoprecipitated from total protein extracts using TOR specific antibodies and co-immunoprecipitation of SnRK1α1 and SnRK2s was assessed by immunodetection with specific antibodies. The experiment was performed once.

Supplementary Fig. 9. SnRK1α1 and SnRK2.2 show similar expression pattern in the root. Left panels, SnRK1α1 and SnRK2.2 are expressed in the primary root (PR) and during lateral root (LR) development. Right panels, SnRK1α1 and SnRK2.2 are highly enriched in the nucleus. Roots were stained with FM4-64. Scale bars, 30 μm. Three independent experiments were performed with similar results.

Supplementary Fig. 10. SnRK1 and SnRK2 kinases interact *in planta*. a, SnRK1α1 and SnRK2s do not co-immunoprecipitate with GFP alone in roots of seedlings grown in 0.5X MS. **b, c,** The interaction between SnRK1α1 and SnRK2 is detected also in extracts from whole seedlings and the interaction is reduced upon a short ABA treatment (40 min, 50 μM). **b**, IPs from *proSnRK1α1::SnRK1α1-GFP* seedlings. GFP blots are the same as in Fig. 1d (right panel; same membrane used to detect TOR and SnRK2); **c,** IPs from *proSnRK2.2::SnRK2.2-GFP* seedlings. Two independent experiments were performed with similar results (**a-c**). **d, e,** Immunoprecipitation of SnRK2.3 and SnRK2.6 using FLAG-tagged overexpressor lines provides further support for the SnRK2-SnRK1α1 interaction in mock and for the decrease of this interaction in ABA (3h, 50 μM). A line overexpressing GFP-FLAG is used as a negative control. Two independent experiments are shown.

Supplementary Fig. 11. SnRK2s interact with SnRK1 in a PP2CA-dependent manner. BiFC experiments show that SnRK1α1 interacts with SnRK2.3 and SnRK2.6 only in the presence of PP2CA and this interaction occurs mostly in the nucleus. A kinase dead SnRK2.6 ($SnRK2.6^{G33R}$) further shows that the SnRK1α1-SnRK2 interaction is not dependent on the

kinase activity of the latter. **a,** Representative pictures of *Nicotiana benthamiana* epidermal cells expressing YFP^N-SnRK1α1 and the indicated YFP^C-SnRK2 with a nuclear localized RFP (mRFP-NLS) or with PP2CA-RFP. Scale bars, 30 µm. **b,** Quantification of RFP and YFP signals (error bars, SEM; mRFP-NLS+SnRK2.3/SnRK2.6, n=13; mRFP-NLS+SnRK2.6^{G33R}, n=12; PP2CA-RFP+SnRK2.3/SnRK2.6^{G33R}, n=7; PP2CA-RFP+SnRK2.6, n=8). **c,** Immunoblot analyses of *Nicotiana benthamiana* leaf sections demonstrate the expression of all indicated proteins. Two independent experiments were performed with similar results.

Supplementary Fig. 12. Generation of the *snrk2d/1α1* mutant. a, Scheme showing the insertion sites of the *snrk1α1, snrk2.2* and *snrk2.3* T-DNA mutations of the parental lines. **b,** Confirmation of the *snrk2d/1α1* mutant identity by genotyping. The *snrk2d/1α1* mutant was generated by crossing the *snrk2d* (*snrk2.2 snrk2.3*) and *snrk1α1-3* mutants. F2 individuals able to grow on 1 µM ABA were genotyped for the *snrk1α1-3* mutation and plants homozygous for *snrk1α1-3* were confirmed to be homozygous for *snrk2.2* and *snrk2.3* by genotyping with the corresponding primers. Three independent analyses were performed with similar results.

Supplementary Fig. 13. SnRK1 is not directly activated by SnRK2.3. a, A *RD29B::LUC* reporter gene assay in Arabidopsis protoplasts demonstrates the activity of transiently expressed SnRK2.3 when cells are treated with ABA. n=2 (REP1, REP2 correspond to two independent experiments). **b,** Anti-HA immunoblot showing the successful immunoprecipitation of the indicated proteins from transfected protoplasts. **c,** *In vitro* kinase assay using phosphorylation of the AMARA peptide as readout of SnRK1 activity shows that purified recombinant SnRK1α1 is only activated by SnAK2 but not by ABA-activated SnRK2.3. Dots correspond to the values from two independent experiments.

Supplementary Fig. 14. SnRK2s are not required for SnRK1 activation in response to energy deficit. a, Repression of TOR signaling in response to a sudden darkness treatment is defective in the *sesquiα2* mutant. Seedlings grown on liquid culture (0.5X MS + 0.5% sucrose) were covered 3h after the onset of the light period and samples were collected at T0, and 1h and 3h of dark treatment. TOR activity was subsequently analyzed from total protein extracts of each sample using immunoblotting and $RPS6^{S240}$ phosphorylation as readout. Two independent experiments are shown. Numbers refer to the decrease in RPS6 phosphorylation

[P(S240)-RPS6/total RPS6)] relative to the T0 (100%). **b,** Repression of TOR signaling in response to a sudden darkness treatment is normal in the *snrk2t* mutant. Graph corresponds to the average of 3 independent experiments (error bars, SEM). ns, not significant (two-tailed Student t-test).

Supplementary Fig. 15. Dual effect of SnRK2.3 overexpression on primary root (PR) growth. In control conditions plants overexpressing SnRK2.3 (SnRK2.3-OE) have increased PR growth compared to the WT. Conversely, the repression of PR growth triggered by ABA is enhanced in the SnRK2.3-OE, in agreement with its known ABA hypersensitivity. Left panel, representative picture of seedlings grown vertically on 0.5X MS medium for 5d and transferred to 0.5X MS with or without ABA for 8d. Bar = 1cm. Right panels, quantification of PR length from 5 independent experiments (total number of plates: WT mock n=58, SnRK2.3-OE mock n=57, WT ABA n=53, SnRK2.3-OE ABA n=52; total number of seedlings: 89-133 per genotype and condition). Upper and lower box boundaries represent the first and third quantiles, respectively, horizontal lines mark the median and whiskers mark the highest and lowest values. *p*-values denote statistically significant differences (two-tailed Student t-test).

SUPPLEMENTARY MATERIALS AND METHODS

A list of all primers and antibodies used in this study is provided in Table S1.

Plant Material

All *Arabidopsis thaliana* plants used in this study are in the Columbia (Col-0) background. Single SnRK1α insertional mutant lines were obtained from the GABI-Kat and WISC public collections[2,3] through the Nottingham Arabidopsis stock center (NASC)*: snrk1α1-3* (GABI_579E09)[4], *snrk1α2-1* (WiscDsLox320B03)[5] and *snrk1α2-2* (WiscDsLox384F5). All other lines were previously described: *snrk2.6* (*ost1*; SALK_008068)[6], *snrk2.2/snrk2.3* (*snrk2d*; GABI-Kat 807G04, SALK_107315)[7], *snrk2.2/snrk2.3/snrk2.6* (*snrk2t*)[8], *proSnRK1α1::SnRK1α1-GFP* (*SnRK1α1-GFP/AKIN10-GFP*)[9], *proSnRK2.2::SnRK2.2-GFP* (*SnRK2.2-GFP*; #2.2)[10], *35S::SnRK2.3*[11], *35S::GFP*[12], *UBQ10::GFP-His-FLAG*[13] and *UBQ10::OST1-His-FLAG*[13].

The *sesquiα2-1* (*snrk1α1-3*$^{-/-}$ *snrk1α2-1*$^{+/-}$) and *sesquiα2-2* (*snrk1α1-3*$^{-/-}$ *snrk1α2-2*$^{+/-}$) mutants were obtained by crossing the *snrk1α1-3* mutant and the *snrk1α2-1* and *snrk1α2-2* mutants,

respectively. For the selection of *sesquiα2* individuals from the segregating *sesquiα2* progeny, seeds were plated on half-strength Murashige and Skoog medium (0.5X MS) supplemented with glufosinate-ammonium (BASTA, 10 mg/L). After 5-6 days of growth, resistant *sesquiα2* individuals were transferred to non-BASTA medium for various assays. All phenotypic assays performed with the *sesquiα2* mutants had as control a BASTA-resistant *35S::GFP* line [referred as Col(B) in the text]. These seedlings were always preselected in BASTA-containing medium, similarly to the *sesquiα2* mutants.

Triple *snrk2.2/snrk2.3/snrk1α1-3* insertional mutants (referred as *snrk2d/α1* in the text) were obtained by crossing *snrk1α1-3* to the *snrk2.2/snrk2.3* double mutant. F2 individuals able to grow on 1 µM ABA were genotyped for the *snrk1α1-3* mutation and plants homozygous for *snrk1α1-3* were confirmed to be homozygous for *snrk2.2* and *snrk2.3* by genotyping with the corresponding primers (see Table S1).

Plant Growth Conditions and Phenotype Assays

Unless otherwise specified, plants were grown under long-day conditions (16h light, 100 µmol $m^{-2}s^{-1}$, 22°C /8h dark, 18°C). Sterilized seeds were sowed on plates containing 0.5X MS medium [0.5X MS (Duchefa M0222.0050) 0.05% MES, 0.8% phytoagar, pH 5.7], sealed with Micropore tape, and stratified in the dark at 4ºC for 2 days before transfer to the growth chamber.

ABA sensitivity during germination and early seedling development

For assays of ABA sensitivity during germination and early seedling development, seeds were plated on 0.5X MS supplemented or not with ABA, and radicle emergence and cotyledon greening were computed over time under a stereoscope. Note that in these assays the *sesquiα2* mutants cannot be identified by pre-selection on BASTA and hence plates contain a mixed population of *sesquiα2* and single *snrk1α1-3* mutants (Confraria *et al*., in preparation).

ABA sensitivity during root development

For assaying ABA sensitivity during root development, seedlings were grown vertically for 5 days in 0.5X MS (allowing the BASTA selection of *sesquiα2* individuals and the control *35S::GFP* line, when needed) and transferred to 0.5X MS plates supplemented or not with ABA. The tip of the root was marked after the transfer and seedlings were allowed to grow vertically for 8 more days before scanning. Scanned images were analyzed using Image J

software (Rasband, W.S., ImageJ, U. S. National Institutes of Health, Bethesda, Maryland, USA, https://imagej.nih.gov/ij/, 1997-2018), to measure primary root (PR) length and to count the number of lateral roots (LRs; cut-off of ≥ 0.5 mm length). All computed parameters relate to the region of the root that developed after the transfer to mock or ABA. LR density = number of LRs/PR length. Quantification was done from a minimum of 32 seedlings (range 32-72) for each genotype and condition and grown at least as 2 independent batches. Average values for all parameters were calculated for each genotype in each plate and these were used as single units for the final quantification (*n* therefore corresponds to the total number of plates used in each experiment).

Effect of light intensity on root growth

For assessing the effect of low light intensity on root growth, seedlings were grown vertically for 7 days in 0.5X MS medium (supplied with BASTA to allow selection of the *sesquiα2* mutant) under normal light conditions (16h light, 100 µmol $m^{-2}s^{-1}$, 22°C /8h dark, 18°C) and transferred to new 0.5X MS plates. The tip of the root was marked after the transfer and seedlings were allowed to grow for 7 more days under low light conditions (16h light, 40 µmol $m^{-2}s^{-1}$, 22ºC/8h dark, 18ºC) or under normal light as a control. Plates were scanned and PR length and LR density were quantified as in *ABA sensitivity during root development.*

Effect of AZD8055 on root growth

For assessing the effect of TOR inhibition by AZD8055, seedlings were grown vertically for 7 days in 0.5X MS medium, and transferred to 0.5X MS medium plates containing either DMSO (<0.005%, mock treatment) or 0.2, 0.5 or 1 µM AZD-8055 (dissolved in DMSO). The tip of the root was marked after the transfer and seedlings were allowed to grow for 7 more days before scanning. PR length was quantified as explained in *ABA sensitivity during root development.*

Water loss assay

For water loss assays plants were grown in soil under a 12h light (100 µmol $m^{-2}s^{-1}$), 22°C/12h dark, 18°C regime. Five leaves of each indicated were detached from five different plants and exposed to the drying atmosphere of a laminar flow hood. Fresh weight was recorded at time zero (T0) and at the indicated time points. Water loss was calculated for each detached leaf as the difference in fresh weight at a specific time point compared to the initial fresh weight. Values are expressed as percentage of the initial fresh weight values.

Gene Expression Analyses

Analyses of SnRK1 marker genes

For confirming impairment of SnRK1 marker gene induction in *sesquiα2-1* and *sesquiα2-2* plants, seedlings were pre-selected in BASTA for 7-10d and transferred to soil, where they grew for 4 weeks under a 12h light (100 µmol $m^{-2}s^{-1}$), 22°C/12h dark, 18°C regime. Rosette leaves were detached and incubated on sterile MilliQ water in covered Petri dishes under light (control; 100 µmol $m^{-2}s^{-1}$) or darkness (energy stress)[14] for 6h (started approx. 3h after lights on). Each sample was composed of 3 leaves pooled from 3 different plants. After treatment, leaves were collected, gently dried, flash frozen in liquid N_2, and stored at -80°C until used.

Analyses of ABA marker genes

For analyses of ABA marker gene induction, 10-day old seedlings from BASTA-selected Col(B) and the *sesquiα2-1* mutant were grown in liquid cultures in 0.5X MS and treated with mock or 50 µM ABA for 3h. Whole seedlings were collected, gently dried, and stored at -80°C until used.

Following the indicated treatments, total RNA was extracted using TRIzol reagent (Life Technologies), treated with RNAse-Free DNAse (Promega) and reverse transcribed (1µg) using Oligo (dT)18 primers and SuperScript III Reverse Transcriptase (Life Technologies). qRT-PCR analyses were performed using an Applied Biosystems Quantstudio 6 real-time PCR instrument employing iTaq Universal SYBR Green Supermix (Biorad) and $2^{-\Delta CT}$ or comparative CT method[15] using for normalization the geometric mean[16] of *EIF4* and *UBQ10* (for SnRK1 marker genes) or *ACT8* (for ABA marker genes).

Protoplast transient expression assays

Vectors for protoplast transient expression and assays were as described, using the *UBQ10-GUS* reporter as transfection efficiency control[17,18]. For constructs for overexpression of SnRK2.3-HA, ABF2-HA, and SnAK2-HA, the corresponding coding sequences were cloned into a pHBT95 vector harboring the indicated C- or N-terminal tag. ABA signaling was monitored using a *RD29B::LUC* reporter assay in protoplasts isolated from the *snrk2t* mutant[19]. ABA was added to a final concentration of 5 µM one hour after transfection and protoplasts were thereafter incubated for 5h. For measurements of LUC and GUS activities samples were processed as previously described[17,18]. For immunoprecipitation, protoplast

transfection was upscaled 5-fold (0.5 mL cells) and processed as described in the section *Immunoprecipitation of proteins expressed in protoplasts.*

Protein interactions

Bimolecular Fluorescence complementation assays

For BiFC experiments, constructs for protein expression were generated using pGWB554[20], and pYFPN43/pYFPC43 vectors[21]. The different binary vectors were introduced into *Agrkobacterium tumefaciens* C58C1 (pGV2260) by electroporation and transformed cells were selected in LB plates supplemented either with spectinomycin (50 µg/mL) and rifampicin (25 µg/mL) in the case of pGWB5544 or kanamycin (50 µg/mL) and rifampicin (25 µg/mL) for the rest of the constructs. Overnight grown cultures of *A. tumefaciens* of about 2.0 OD600 units were collected and resuspended in infiltration buffer (10 mM $MgCl_2$, 10 mM MES pH 5.6, 200 µM acetosyringone) and incubated for 3 to 5 hours at room temperature in a rocking platform. A mixture of *A. tumefaciens* strains containing the fluorescent translational fusion constructs and the p19 plasmid (pCH32 35S:p19) expressing the silencing suppressor p19 of tomato bushy stunt[22] was prepared for co-infiltration so that the final density of each *A. tumefaciens* culture was 0.75. Young fully expanded leaves of 4-week old *Nicotiana benthamiana* plants were transformed by infiltration into the abaxial air space with a needleless syringe. Leaves were examined 72-96 h after infiltration using confocal laser scanning microscopy.

Confocal imaging was performed using a Zeiss LSM 780 AxioObserver.Z1 laser scanning microscope with a C-Apochromat 403/1.20 W corrective water immersion objective lens. The following fluorophores were used at the indicated wavelengths: YFP (488 nm/495 to 530 nm), RFP (561 nm/605 to 670). For the experiments involving multi-colour detection of two fluorescent proteins, sequential imaging of the fluorescent proteins was performed using the sequential channel acquisition mode. Pinholes were adjusted to 1 Air Unit for each wavelength. For the YFP quantitative analysis the power of the 488 nm laser was set at 2.0% transmission to gain master of 700. Post-acquisition image processing and fluorescence quantification was performed using ImageJ (http://rsb.info.gov/ij/).

Co-immunoprecipitation of SnRKs with TOR and RAPTOR

For immunoprecipitation of SnRKs, Arabidopsis *proSnRK1α1::SnRK1α1-GFP*, *proSnRK2.2::SnRK2.2-GFP* and *35S::GFP* seedlings were grown vertically during 7 days in

solid 0.5XMS + 0.5% sucrose and transferred to liquid 0.5X MS + 0.5% sucrose where they grew for the following 7 days (60 seedlings per 100 mm x 25 mm plate containing 10 mL of medium). Medium was refreshed 8h before the start of the last night and the day after seedlings were treated or not for 40 min with 50 µM ABA (by adding directly the hormone into the refreshed medium 5h after the onset of the lights). Whole seedling protein extracts were thereafter prepared for co-IP experiments (roughly 180 seedlings per IP). Briefly, samples were collected, ground in liquid nitrogen and immediately placed in IP buffer [50 mM Tris-HCl pH 8.0, 150 mM NaCl, 0.1% NP-40, 3 mM DTT, 50 µM MG-132, Phosphatase Inhibitor Cocktails 2 and 3 (Sigma; 20 µL each per 10 mL of IP buffer) and cOmplete™ Protease Inhibitor Cocktail (Roche, 1 tablet per 10 mL of IP buffer)] on ice for protein extraction (9 mL of IP buffer per 6 g of ground tissue). Homogenates were cleared by centrifugation at 12000 g for 15 minutes at 4°C, and supernatants were used for immunoprecipitation (20 mg). SnRK1α1-GFP, SnRK2.2-GFP, or GFP proteins were immunoprecipitated using super-paramagnetic µMAC beads coupled to monoclonal anti-GFP antibody (Miltenyi Biotec; 100 µL slurry per 20 mg of total protein in a final volume of 8 mL) by gentle rocking at 4°C for 3h. Purified immunocomplexes were eluted in Laemmli buffer, boiled and run in an 8% SDS-PAGE gel. Each input (50 µg) and the proteins immunoprecipitated with anti-GFP antibody (the entire eluate) were analyzed by Western Blot using anti-GFP, anti-TOR, anti-RAPTOR, anti-SnRK1α1, and anti-SnRK2 antibodies.

For immunoprecipitation of endogenous TOR Arabidopsis seedlings were grown vertically on solid 0.5X MS + 0.5% sucrose for 7 days and transferred to liquid 0.5X MS + 0.5% sucrose where they grew for the following 7 days. Medium was refreshed 8h before the start of the last night and the day after seedlings were treated or not for 40 min with 50 µM ABA (by adding directly the hormone into the refreshed medium 5h after the onset of the lights). Whole seedling protein extracts were thereafter prepared for co-IP experiments (roughly 180 seedlings per IP). Briefly, samples were collected, ground in liquid nitrogen and immediately placed in IP buffer [50 mM Tris-HCl pH 8.0, 150 mM NaCl, 0.1% NP-40, 3 mM DTT, 50 µM MG-132, Phosphatase Inhibitor Cocktails 2 and 3 (Sigma; 20 µL each per 10 mL of IP buffer) and cOmplete™ Protease Inhibitor Cocktail (Roche, 1 tablet per 10 mL of IP buffer)] on ice for protein extraction (9 mL of IP buffer per 6 g of ground tissue). Homogenates were cleared by centrifugation at 12000 g, 4ºC for 15 min, and supernatants were used for immunoprecipitation (20 mg). TOR was immunoprecipitated from each extract with 20 µL of anti-TOR antibody for 4h at 4°C with gentle rocking. To this end, 80 µL of Dynabeads™

Protein A (Invitrogen™) were pre-washed twice with 200 µL of IP buffer by using the DynaMag™ Magnet system (Invitrogen™) and coupled during 2h at 4ºC in gentle agitation with 20 µL of anti-TOR antibody premixed with 200 µL of IP buffer. Samples were washed 4 times with 400 µL of IP Buffer using the DynaMag™ Magnet and purified immunocomplexes were eluted in 70 µL 2x Laemmli buffer after boiling 15 min at 95°C. Each input (50 µg) and the proteins immunoprecipitated with anti-TOR antibodies (the entire eluate) were separated in a 8% SDS-PAGE gel and analyzed by Western blot with anti-TOR, anti-SnRK1α1, and anti-SnRK2s antibodies.

Co-immunoprecipitation of SnRK1 with SnRK2 and PP2CA

Arabidopsis *proSnRK1α1::SnRK1α1-GFP*, *proSnRK2.2::SnRK2.2-GFP* and *35S::GFP* seedlings were grown vertically during 7 days in solid 0.5X MS + 0.5% sucrose and transferred to liquid 0.5X MS + 0.5% sucrose where they grew for the following 7 days (60 seedlings per 100 mm x 25 mm plate containing 10 mL of medium). Medium was refreshed 8h before the start of the last night and the day after seedlings were treated or not for 3h with 50 µM ABA (by adding directly the hormone into the refreshed medium 5h after the onset of the lights). Roots were rapidly collected, flash frozen in liquid nitrogen and stored in -80 °C until usage (900 mg of ground roots collected from roughly 180 seedlings per IP). Frozen root samples were ground in liquid nitrogen to a fine powder and immediately placed in IP buffer (50 mM Tris-HCl pH 8.0, 150 mM NaCl, 1% Triton X-100, 3 mM DTT, 50 µM MG-132, Phosphatase Inhibitor Cocktails 2 and 3 - Sigma (20 µL each per 10 mL of IP buffer) and cOmplete™ Protease Inhibitor Cocktail – Roche, 1 tablet per 10 mL of IP buffer) on ice for protein extraction (1.4 mL of IP buffer per 900 mg of ground root tissue). Homogenates were cleared by centrifugation at 12000 g for 15 minutes at 4° C and supernatants were recovered for immunoprecipitation. Soluble proteins were quantified using Bradford solution and 2 mg of total proteins were used to immunoprecipitate GFP tagged proteins using super-paramagnetic µMACS beads coupled to monoclonal anti-GFP antibody (Miltenyi Biotec; 50 µL slurry of beads per 2 mg of total protein in 1.2 mL of final volume) by gentle rocking at 4°C for 3h. Purified immunocomplexes were eluted in Laemmli buffer, boiled and run in a 12% SDS-PAGE gel. Each input (20 µg) and the proteins immunoprecipitated with anti-GFP antibody (the entire eluate) were analyzed by Western Blot using anti-GFP, anti-SnRK1α1, anti-SnRK2, and anti-PP2CA antibodies[23]. When indicated, the SnRK1-SnRK2 interaction was analyzed also from whole seedlings following a 40 min treatment with 50 µM ABA.

Immunoprecipitation in this case was performed as in *Co-immunoprecipitation of SnRKs with TOR and RAPTOR.*

Co-immunoprecipitation of SnRK1α1 with SnRK1β1

For immunoprecipitation of endogenous SnRK1α1 Arabidopsis Col-0 seedlings were grown vertically on solid 0.5X MS + 0.5% sucrose for 7 days and transferred to liquid 0.5X MS + 0.5% sucrose where they grew for the following 7 days. Medium was refreshed 8h before the beginning of the night and the following day seedlings were collected 6h after the onset of the lights. Whole seedling protein extracts were thereafter prepared for co-IP experiments (roughly 150 seedlings per IP). Briefly, samples were ground in liquid nitrogen and immediately placed in IP buffer [50 mM Tris-HCl pH 8.0, 150 mM NaCl, 0.1% NP-40, 3 mM DTT, 50 µM MG-132, Phosphatase Inhibitor Cocktails 2 and 3 (Sigma; 20 µL each per 10 mL of IP buffer) and cOmplete™ Protease Inhibitor Cocktail (Roche, 1 tablet per 10 mL of IP buffer)] on ice for protein extraction (6 mL of IP buffer per 4 g of ground tissue). Homogenates were cleared by centrifugation at 12000 g, 4ºC for 15 min, and supernatants (totaling 15 mg of protein) were used for immunoprecipitation. SnRK1α1 was immunoprecipitated from each extract with 25 µg of anti-SnRK1α1 commercial antibody (Agrisera AS10 919), for 4h at 4°C with gentle rocking. To this end, anti-SnRK1α1 antibodies were previously coupled with 3 mg (100 µL) of Dynabeads® M-270 Epoxy by means of the Dynabeads® Antibody Coupling Kit (Catalog number 14311D, Life Technologies™) following the manufacturer´s instructions. Samples were washed 4 times with 400 µL of IP Buffer using the DynaMag™ Magnet and purified immunocomplexes were eluted in 70 µL of preboiled (15 min at 95°C) 2x Laemmli buffer. Each input (100 µg) and the proteins immunoprecipitated with anti-SnRK1α1 antibodies (the entire eluate) were separated in one 8% SDS-PAGE gel and analyzed by Western blot with anti-SnRK1α1, and anti-SnRK1β1 antibodies.

Immunoprecipitation of proteins expressed in protoplasts

Immunoprecipitation was performed from 0.5 mL of transfected mesophyll protoplasts expressing the indicated HA-tagged proteins, harvested and flash-frozen. Frozen protoplast pellets were mixed with 200 µL of IP buffer [50 mM Tris-HCl pH 8.0, 150 mM NaCl, 1 mM EDTA, 0.3% NP-40, 3 mM DTT, 50 µM MG-132, Phosphatase Inhibitor Cocktails 2 and 3 (Sigma; 20 µL each per 10 mL of IP buffer) and cOmplete™ Protease Inhibitor Cocktail (Roche, 1 tablet per 10 mL of IP buffer)] on ice for protein extraction. HA-tagged proteins

were immunoprecipitated using 25 µL of super-paramagnetic µMAC beads coupled to monoclonal anti-HA antibody (Miltenyi Biotec) by gentle rocking at 4°C for 2h. After incubation, immunoprecipitated HA-tagged proteins were trapped in the column using a MACS™ Separation Columns (Miltenyi Biotec) where they were washed 4 times with 200-300 µL of IP Buffer. Purified immunoprecipitated HA-tagged proteins still joined to the super-paramagnetic µMAC beads were eluted with 30 µL of IP buffer twice. Samples were divided in aliquots of 15 µL, flash-frozen in liquid nitrogen and stored at -20ºC. One aliquot of each sample was used for Western blot and immunodetection analyses and another for *in vitro* kinase assays.

RPS6^{S240} phosphorylation assays

Seedlings were grown vertically for 6 days in 0.5X MS + 0.5% sucrose medium [when required, also supplemented with BASTA to allow selection of Col(B) and *sesquiα2* individuals] and transferred to 6-well plates containing 0.5X MS liquid medium supplemented with 0.5% sucrose for 6 more days (10 seedlings per 9.5 cm^2 well containing 1 mL of medium).

ABA and TOR inhibitors

For confirming the effect of ABA and TOR inhibitors on RPS6^{S240} phosphorylation as readout of TOR signaling, the liquid medium was refreshed 8h before the beginning of the last night and the day after seedlings were mock-treated or treated with 50 µM ABA, 10 µM torin2 or 2 µM AZD during 4h (by adding directly the hormone into the refreshed medium 3h after the onset of the lights).

ABA time course

For comparing the ability of the indicated genotypes to repress RPS6^{S240} phosphorylation in response to ABA, the liquid medium was refreshed 8h before the beginning of the last night. On the following day samples were collected 1h after the onset of the lights (T0) and the remaining seedlings were treated with 50 µM ABA for 15 min, 30 min, 45 min, 1 h and 4h (by adding directly the hormone into the refreshed medium 3h after the onset of the lights).

Nutrient supplementation time course

For comparing the ability of the indicated genotypes to induce RPS6^{S240} phosphorylation in response to nutrient supplementation, T0 samples were collected on the 7th day of growth on

liquid 1h after the onset of the lights. Thereafter the growth medium of the remaining seedlings was replaced with fresh medium and seedlings were collected after 30, 60 and 180 min.

Dark treatment

For comparing the ability of the indicated genotypes to repress RPS6^{S240} phosphorylation in response to sudden darkness, the medium was refreshed 8h before the beginning of the last night. On the following day samples were collected 3h after the onset of the lights (T0) and the remaining seedlings were transferred to darkness for 1 or 3h to induce energy stress.

Following the indicated treatments, samples were ground to a fine powder in liquid nitrogen and immediately placed in extraction buffer [50 mM Tris-HCl pH 8.0, 150 mM NaCl, 1% Triton X-100, 3 mM DTT, 50 µM MG-132, Phosphatase Inhibitor Cocktails 2 and 3 (Sigma, 20 µL each per 10 mL of buffer) and cOmplete™ Protease Inhibitor Cocktail (Roche 1 tablet per 10 mL of buffer)] for total protein extraction (150 µL of buffer per 100 mg of ground tissue). Homogenates were cleared by centrifugation at 12000 g for 15 minutes at 4°C and supernatants were recovered for subsequent analyses. 50 µg of total protein extract of each sample were analyzed by Western Blot with anti-phospho-RPS6^{S240} and anti-RPS6 antibodies[24].

Phosphorylation status of TPS5

For assaying the phosphorylation status of TPS5, phosphorylated proteoforms were separated from the non-phosphorylated ones using a Phos-tag gel [25]. For this purpose, seedlings were grown on vertical 0.5X MS plates for 6 days, transferred to fresh 0.5X MS plates, and grown for 9 more days. Then, seedlings were collected 5h after the onset of the lights and flash frozen in liquid nitrogen. For protein extract preparation, each sample was ground in liquid nitrogen to a fine powder and immediately placed in IP buffer (50 mM Tris-HCl pH 8.0, 150 mM NaCl, 1% Triton X-100, 3 mM DTT, 50 µM MG-132, Phosphatase Inhibitor Cocktails 2 and 3 - Sigma (20 µL each per 10 mL of IP buffer) and cOmplete™ Protease Inhibitor Cocktail – Roche, 1 tablet per 10 mL of IP buffer) on ice for protein extraction (150 µL of IP buffer per 100 mg/~6 seedlings of ground tissue). Homogenates were cleared by centrifugation at 12000 g for 15 minutes at 4° C and supernatants were recovered for separation in Phos-tag gel. For this, 100 µg of each protein extract were mixed with 1 mM $MnCl_2$ and proteins were separated in a 6% SDS-PAGE (containing 25 µM Phos-tag™ AAL-

107, 50 µM $MnCl_2$) for 4h at 80V at 4ºC with a magnetic stirrer. Afterwards, gels were washed twice with 1 mM EDTA in transfer buffer for 10 min and once with transfer buffer for another 10 min. Then, separated proteins were analyzed with anti-TPS5 antibodies by Western blot (see below).

Immunoblot analyses

For extraction of total protein for immunoblot analyses, samples were processed as described for *Co-immunoprecipitation of SnRK1 with SnRK2 and PP2CA,* except for analyses of *snrk1α1* single and *sesquiα1* mutants where the following extraction buffer was used: 50 mM Tris-HCl pH7.5, 1 mM EDTA, 150 mM NaCl, 0.05% Triton X-100, 1x cOmplete™ protease inhibitor cocktail, 0.002% Phosphatase Inhibitor Cocktails 2 and 3.

For immunoblotting, proteins were transferred to PVDF membranes for 90 min 110V at 4°C using a wet blotting transfer system – Bio-Rad (transfer buffer 192 mM glycine, 25 mM Tris, 0.1% SDS, 20% ethanol). For immunoblotting Phos-tag gels, proteins were wet transferred overnight at 20V at 4°C. For immunoblotting TOR, proteins were transferred overnight 20V at 4°C using a modified transfer buffer (192 mM glycine, 25 mM Tris, 10% ethanol). Membranes were blocked for at least 1h (5% w/v nonfat dry milk in 1X TBS, 0.05% Tween®) and then incubated with the relevant primary antibody under gentle rocking overnight at 4°C. Secondary antibodies conjugated with horseradish peroxidase (Jackson ImmunoResearch) were used at 1:20000 in 5% non-fat milk in TBS for 1h at RT. For detection of proteins co-immunoprecipitated with endogenous TOR a Veriblot HRP-conjugated secondary antibody (Abcam) was used (1:2000 in 5% milk, 2h incubation). For detection of proteins co-immunoprecipitated with endogenous SnRK1α1 an anti-rabbit light chain HRP-conjugated secondary antibody (Jackson ImmunoResearch) was used (1:20000 in 5% milk, 2h incubation). Images were aquired using ChemiDoc system (Biorad) equipped with a CCD camera.

Production and Purification of Recombinant Proteins

Polyhistidine-tagged SnRK1α1 recombinant protein was produced and purified from Rosetta (DE3) cells. A 500 mL culture (initially inoculated with 5 mL of saturated culture) was grown at 28ºC to 0.5 OD600 and then transferred to 16º C for 1 hour before induction with 1 mM IPTG and O/N (16h) growth. After centrifugation (15 min; 3000g; 4ºC) the pellet was washed with 200 mL 1x PBS buffer, centrifuged again (15 min; 3000g; 4ºC), resuspended in 10 mL

of ice-cold Lysis buffer [50 mM Tris-HCl (pH 8.0); 250 mM KCl; 0.1% Tween-20; 10 % Glycerol; 10 mM Imidazole; 10 mM β-mercaptoethanol; 1 tablet cOmplete™ EDTA-free Inhibitor cocktail (Roche; 1 tablet/50 mL)] and flash-frozen in liquid nitrogen. For protein extraction the frozen pellet was thawed-frozen twice and after resuspension cells were sonicated on ice (30"ON/30"OFF for 5 min), and centrifuged (30 min; 30000g; 4ºC). The supernatant was filtered (Acrodisc® Syringe Filter with Supor® Membrane - 0.45 µm) and applied twice into a gravity column loaded with 2 mL of Ni-NTA resin (Invitrogen™ Ni-NTA Agarose) pre-equilibrated with lysis buffer. The column was washed with 100 mL of ice-cold washing buffer [50 mM Tris-HCl (pH 8.0); 250 mM KCl; 0.1% Tween-20; 10 % Glycerol; 30 mM Imidazole; 10 mM β-mercaptoethanol] and the purified proteins were eluted with elution buffer [50 mM Tris-HCl (pH 8.0); 250 mM KCl; 0.1% Tween-20; 10 % Glycerol; 250 mM Imidazole; 10 mM β-mercaptoethanol] in 8 fractions of 500 µL. Fractions with a protein concentration above 0.85 µg/µL were pooled, dialysed O/N at 4ºC in dialysis buffer [50 mM Tris-HCl (pH 8.0); 100 mM KCl], aliquoted, flash frozen and stored at -80ºC.

Kinase Activity Assay

2 µL of recombinant SnRK1α1 (0.8-1 µg) were incubated with 15 µL of either SnAK2 or SnRK2 proteins immunoprecipitated from transfected mesophyll protoplasts from *A. thaliana* in kinase activity buffer [0.1 M Hepes pH7.25; 10 mM MgCl2; 0.5 mM DTT; 0.5 mM EDTA; 1µL of antiprotease mixture (P9599, Sigma) for 1 mL of buffer; 1 µL of each antiphosphatase mixture (P2850 and P5726, Sigma) for 1 mL of buffer; 20 µM cold ATP] for 1 h at 30º C in a total volume of 22 µL. A 13 µL solution containing 2 µCi of γ-^{32}P ATP (BLU002250UC, PerkinElmer) and 90 µM AMARA peptide (AMARAASAAALARRR) in kinase activity buffer was then added. Following a second incubation for 1 hour at 30º C, the 35 µL were spotted onto 9 cm^2 of Whatman P81 cation-exchange paper. The papers were air dried for 15 min, washed once for 10 min and then twice for 5 min in 200 mL of 1% H_3PO_4 and air dried again for 20 min. ^{32}P incorporation into the AMARA peptide was counted using a scintillation spectrometer (LS6500; Beckman-Coulter) in 4,5 mL of scintillation cocktail liquid (Optiphase Hifase 3 – Perkin Elmer).

Custom-made SnRK1α1 and SnRK1α2 antibodies

Polyclonal *Arabidopsis* SnRK1α1 and SnRK1α2 antibodies were obtained by conjugating synthetic peptides (CTMEGTPRMHPAESVA and CTTDSGSNPMRTPEAGA, respectively; produced by Cocalico Biologicals, Inc. USA) to keyhole limpet hemocyanin and injecting two

rabbits (performed by Cocalico Biologicals). Antibodies were affinity-purified using the original peptides linked to a SulfoLink matrix (Pierce) following instructions by the manufacturer.

Confocal microscopy

The localization of SnRK1α1 and SnRK2.2 was investigated in roots of *proSnRK1α1::SnRK1α1-GFP* and *proSnRK2.2::SnRK2.2-GFP* transgenic lines grown vertically on 0.5X MS plates for 4 (primary roots) or 9 days (lateral roots). Roots were stained with 2 µM FM4-64 for 5 min. Confocal imaging was performed using a Zeiss LSM 780 AxioObserver.Z1 laser-scanning microscope with C-Apochromat 40x/1.20 W corrective water immersion objective. Pinholes were adjusted to 1 Air Unit for each wavelength (GFP, 488 nm/500-530 nm; FM4-64, 488 nm/610-630 nm). Post-acquisition image processing was performed using ZEN (ZEISS Efficient Navigation) Lite 2012 imaging software and ImageJ (http://rsb.info.gov/ij/).

Chemicals

Stocks of ABA (Duchefa Biochemie A0941; 10 mM stock in 50 mM Tris-HCl pH 8.5), Torin 2 (LC Laboratories, MA USA T8448; 10 mM stock in DMSO), AZD8055 (LC Laboratories, MA USA A2345; 20 mM stock in DMSO), BASTA (Sigma 45520; 10 mg/mL in water) were prepared and stored at -20C and used at the indicated concentrations.

Statistical analysis

Basic data processing was performed in Excel. Statistical analyses were performed using GraphPad Prism version 8.4.0 for Windows, GraphPad Software, La Jolla California USA.

REFERENCES

1 Ramon, M. *et al.* Default Activation and Nuclear Translocation of the Plant Cellular Energy Sensor SnRK1 Regulate Metabolic Stress Responses and Development. *Plant Cell* **31**, 1614-1632, (2019).

2 Kleinboelting, N., Huep, G., Kloetgen, A., Viehoever, P. & Weisshaar, B. GABI-Kat SimpleSearch: new features of the Arabidopsis thaliana T-DNA mutant database. *Nucleic Acids Res* **40**, D1211-1215, (2012).

3 Woody, S. T., Austin-Phillips, S., Amasino, R. M. & Krysan, P. J. The WiscDsLox T-DNA collection: an arabidopsis community resource generated by using an improved high-throughput T-DNA sequencing pipeline. *J Plant Res* **120**, 157-165, (2007).

4 Mair, A. *et al.* SnRK1-triggered switch of bZIP63 dimerization mediates the low-energy response in plants. *Elife* **4**, (2015).

5 Jeong, E. Y., Seo, P. J., Woo, J. C. & Park, C. M. AKIN10 delays flowering by inactivating IDD8 transcription factor through protein phosphorylation in Arabidopsis. *BMC Plant Biol* **15**, 110, (2015).
6 Mustilli, A. C., Merlot, S., Vavasseur, A., Fenzi, F. & Giraudat, J. Arabidopsis OST1 protein kinase mediates the regulation of stomatal aperture by abscisic acid and acts upstream of reactive oxygen species production. *Plant Cell* **14**, 3089-3099, (2002).
7 Fujii, H., Verslues, P. E. & Zhu, J. K. Identification of two protein kinases required for abscisic acid regulation of seed germination, root growth, and gene expression in Arabidopsis. *Plant Cell* **19**, 485-494, (2007).
8 Fujii, H. & Zhu, J. K. Arabidopsis mutant deficient in 3 abscisic acid-activated protein kinases reveals critical roles in growth, reproduction, and stress. *Proc Natl Acad Sci USA* **106**, 8380-8385, (2009).
9 Bitrian, M., Roodbarkelari, F., Horvath, M. & Koncz, C. BAC-recombineering for studying plant gene regulation: developmental control and cellular localization of SnRK1 kinase subunits. *Plant J* **65**, 829-842, (2011).
10 Dietrich, D. *et al.* Root hydrotropism is controlled via a cortex-specific growth mechanism. *Nat Plants* **3**, 17057, (2017).
11 Cheng, C. *et al.* SCFAtPP2-B11 modulates ABA signaling by facilitating SnRK2.3 degradation in Arabidopsis thaliana. *PLoS Genet* **13**, e1006947, (2017).
12 Crozet, P. *et al.* SUMOylation represses SnRK1 signaling in Arabidopsis. *Plant J* **85**, 120-133, (2016).
13 Waadt, R. *et al.* Identification of Open Stomata1-Interacting Proteins Reveals Interactions with Sucrose Non-fermenting1-Related Protein Kinases2 and with Type 2A Protein Phosphatases That Function in Abscisic Acid Responses. *Plant Physiol* **169**, 760-779, (2015).
14 Baena-Gonzalez, E., Rolland, F., Thevelein, J. M. & Sheen, J. A central integrator of transcription networks in plant stress and energy signalling. *Nature* **448**, 938-942, (2007).
15 Livak, K. J. & Schmittgen, T. D. Analysis of relative gene expression data using real-time quantitative PCR and the 2(-Delta Delta C(T)) Method. *Methods* **25**, 402-408, (2001).
16 Vandesompele, J. *et al.* Accurate normalization of real-time quantitative RT-PCR data by geometric averaging of multiple internal control genes. *Genome Biol* **3**, RESEARCH0034, (2002).
17 Confraria, A. & Baena-Gonzalez, E. Using Arabidopsis Protoplasts to Study Cellular Responses to Environmental Stress. *Methods Mol Biol* **1398**, 247-269, (2016).
18 Yoo, S. D., Cho, Y. H. & Sheen, J. Arabidopsis mesophyll protoplasts: a versatile cell system for transient gene expression analysis. *Nat Protoc* **2**, 1565-1572, (2007).
19 Fujii, H. *et al.* In vitro reconstitution of an abscisic acid signalling pathway. *Nature* **462**, 660-664, (2009).
20 Nakagawa, T. *et al.* Improved Gateway binary vectors: high-performance vectors for creation of fusion constructs in transgenic analysis of plants. *Biosci Biotechnol Biochem* **71**, 2095-2100, (2007).
21 Belda-Palazon, B. *et al.* Aminopropyltransferases involved in polyamine biosynthesis localize preferentially in the nucleus of plant cells. *PLoS One* **7**, e46907, (2012).
22 Voinnet, O., Rivas, S., Mestre, P. & Baulcombe, D. An enhanced transient expression system in plants based on suppression of gene silencing by the p19 protein of tomato bushy stunt virus. *Plant J* **33**, 949-956, (2003).
23 Wu, Q. *et al.* Ubiquitin Ligases RGLG1 and RGLG5 Regulate Abscisic Acid Signaling by Controlling the Turnover of Phosphatase PP2CA. *Plant Cell* **28**, 2178-2196, (2016).
24 Dobrenel, T. *et al.* The Arabidopsis TOR Kinase Specifically Regulates the Expression of Nuclear Genes Coding for Plastidic Ribosomal Proteins and the Phosphorylation of the Cytosolic Ribosomal Protein S6. *Front Plant Sci* **7**, 1611, (2016).

25 Kinoshita, E., Kinoshita-Kikuta, E. & Koike, T. Phos-tag SDS-PAGE systems for phosphorylation profiling of proteins with a wide range of molecular masses under neutral pH conditions. *Proteomics* **12**, 192-202, (2012).

Supplementary Figure 1

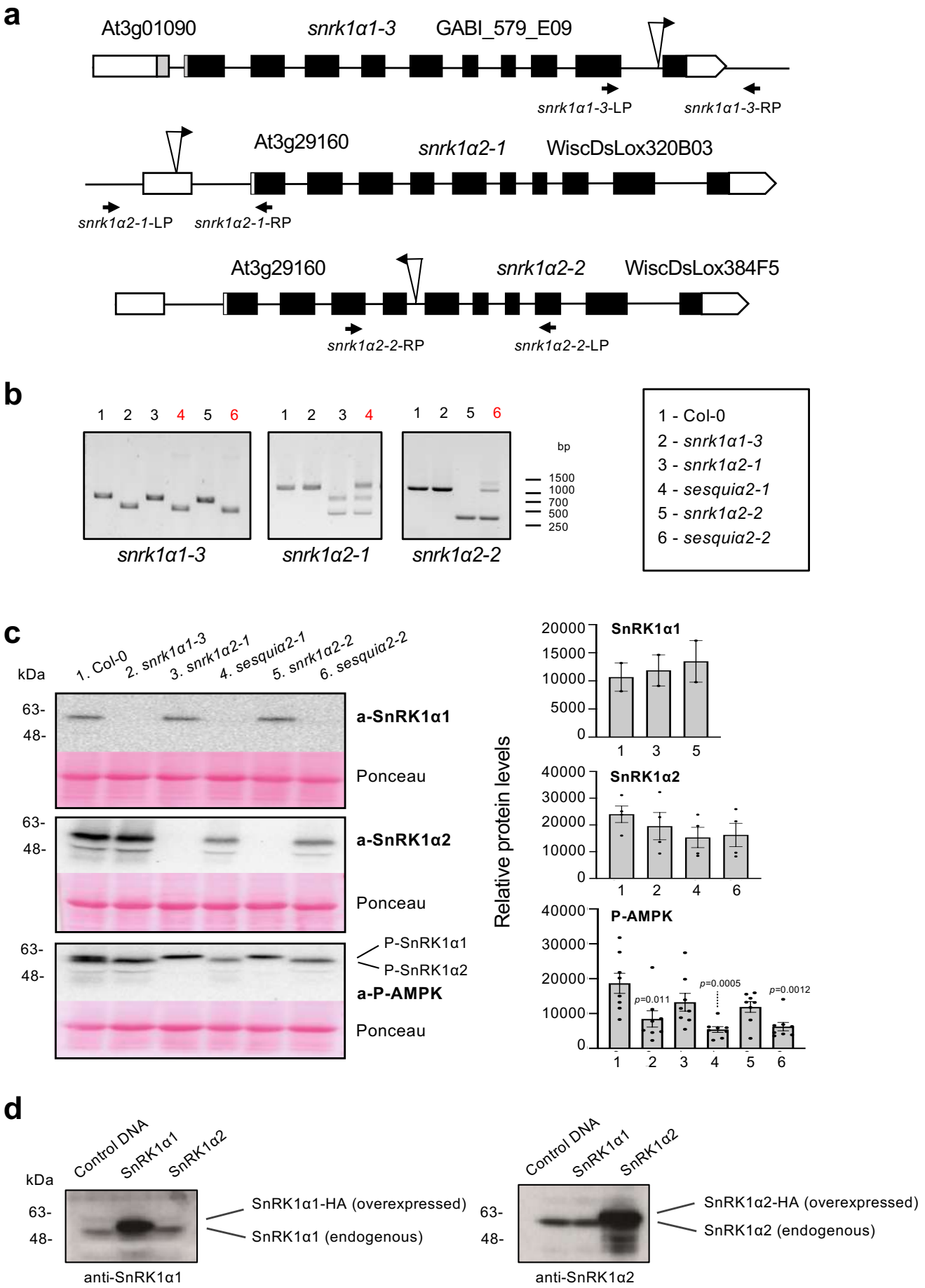

Supplementary Figure 2

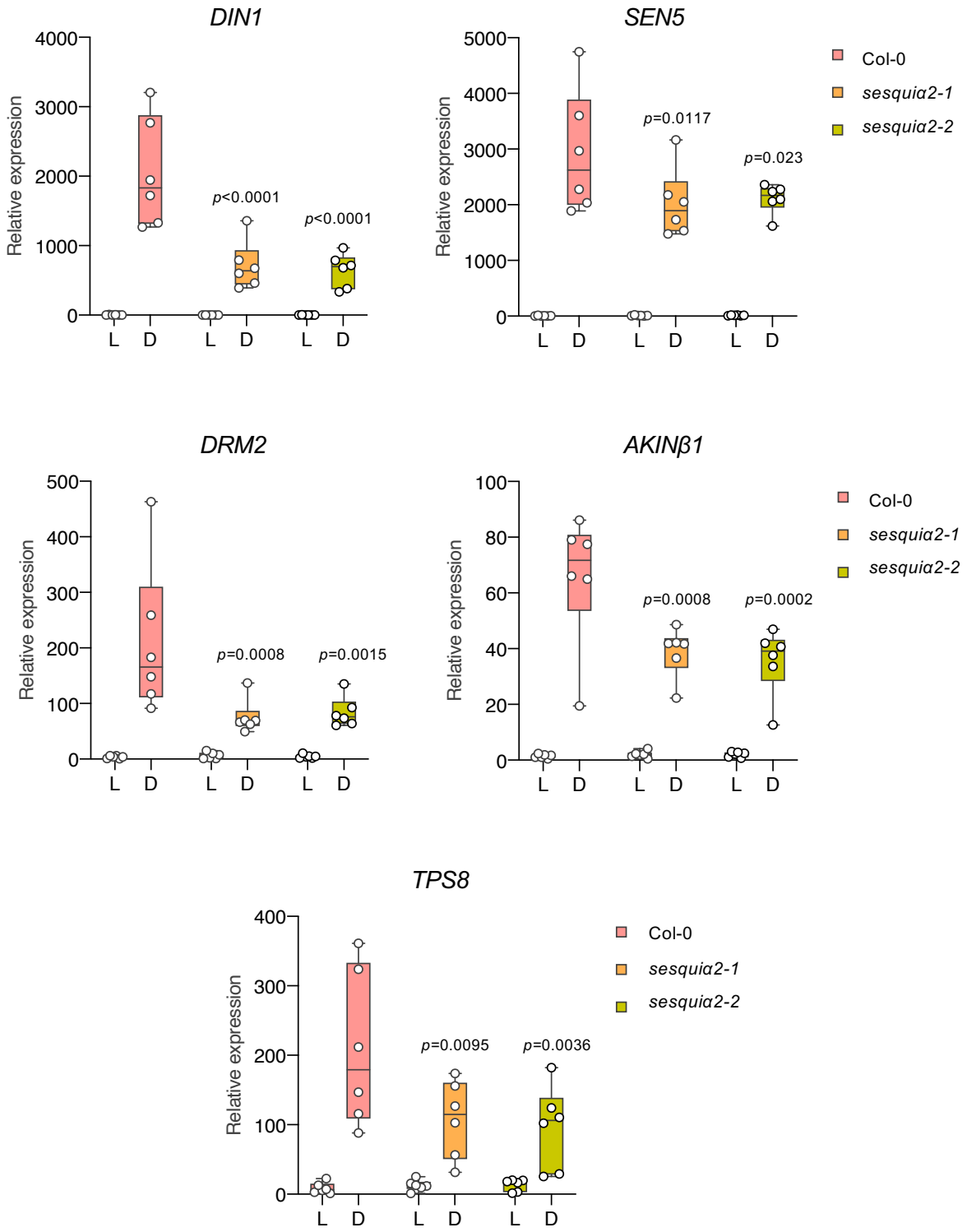

Supplementary Figure 3

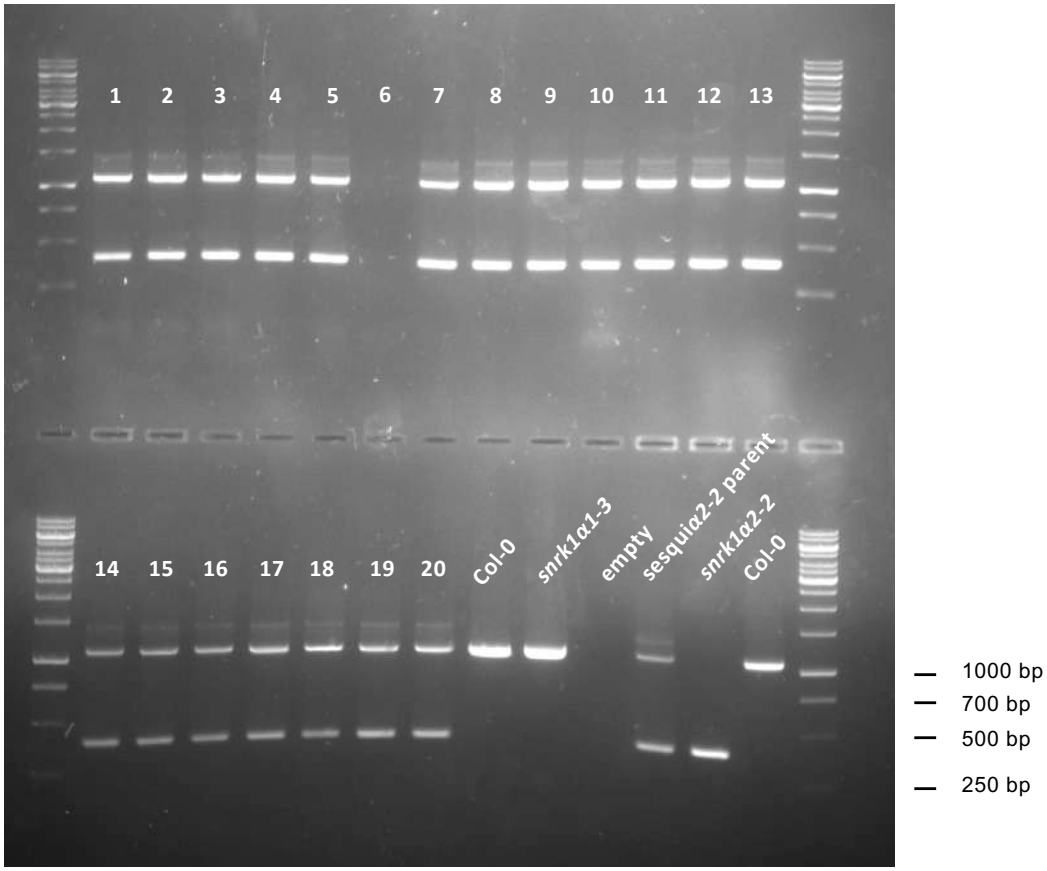

Supplementary Figure 4

a

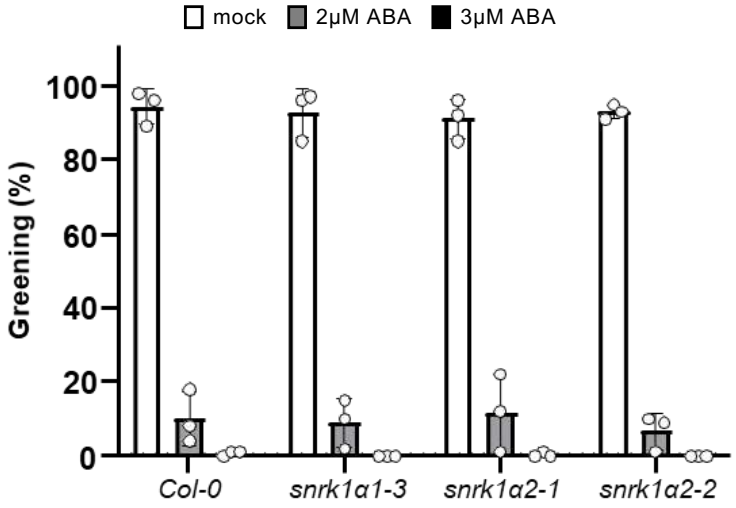

b

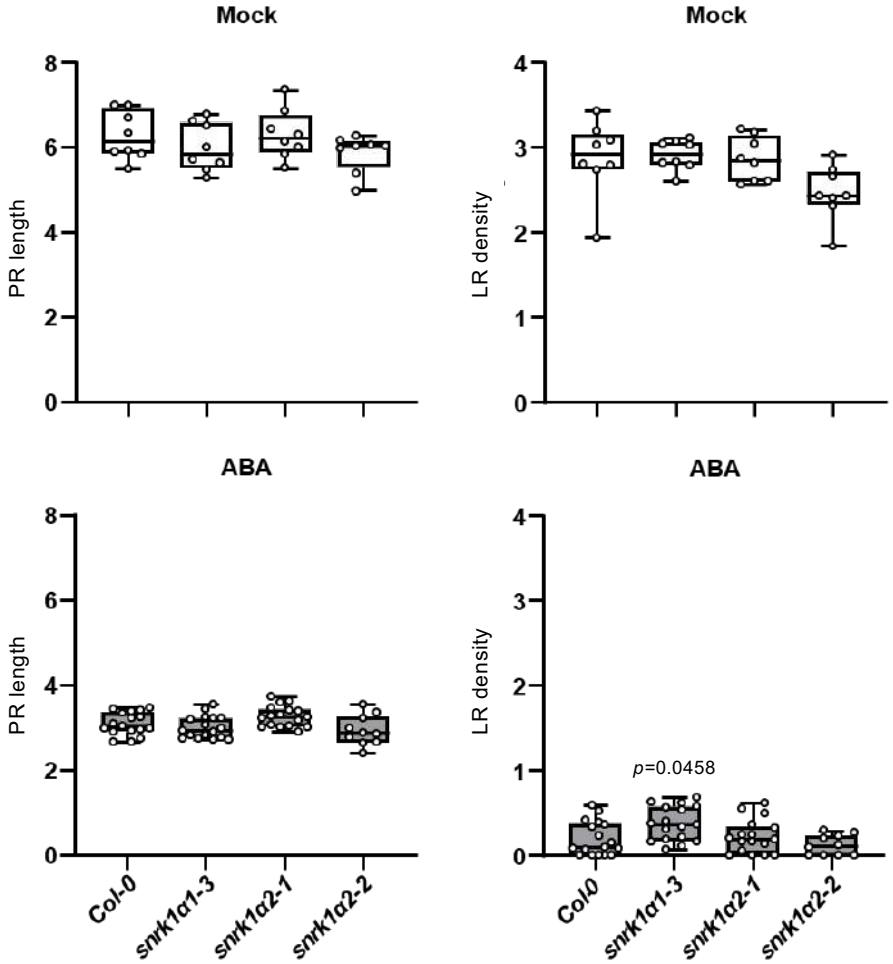

Supplementary Figure 5

a

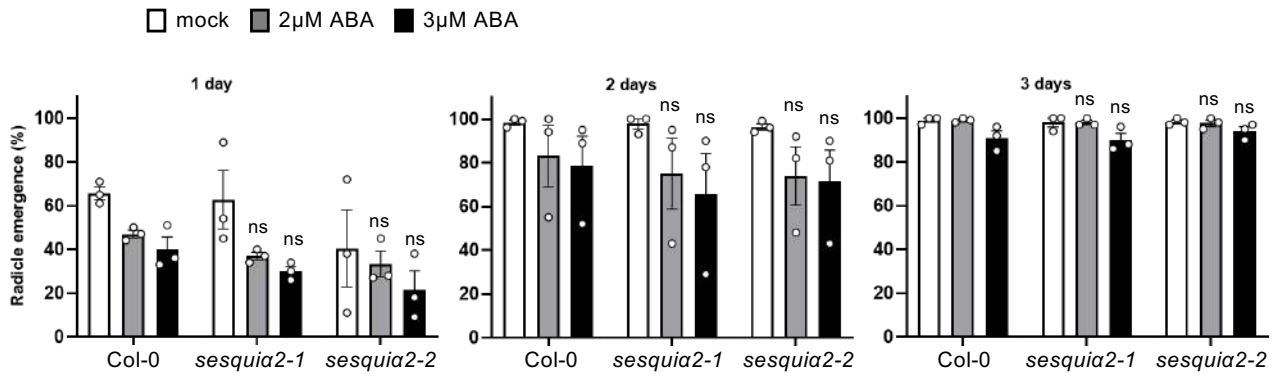

b

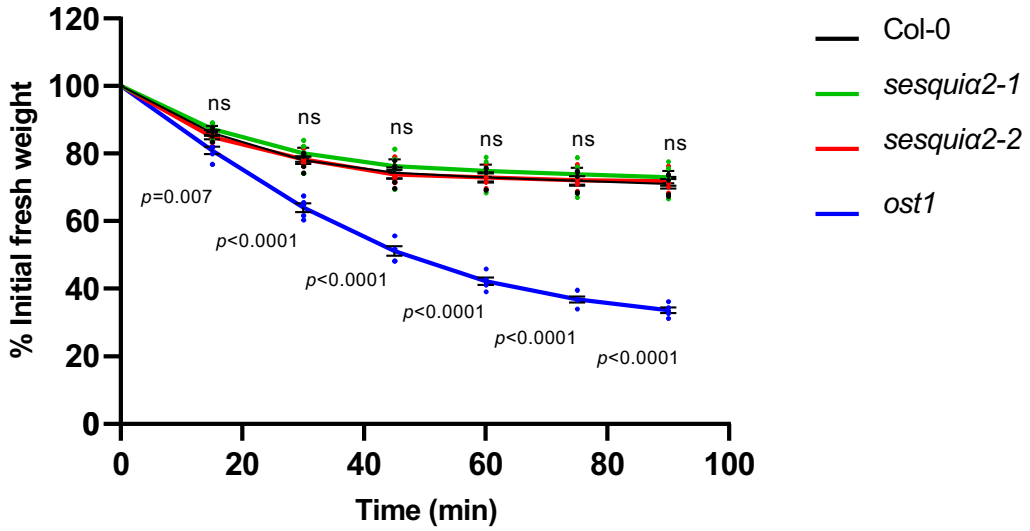

c

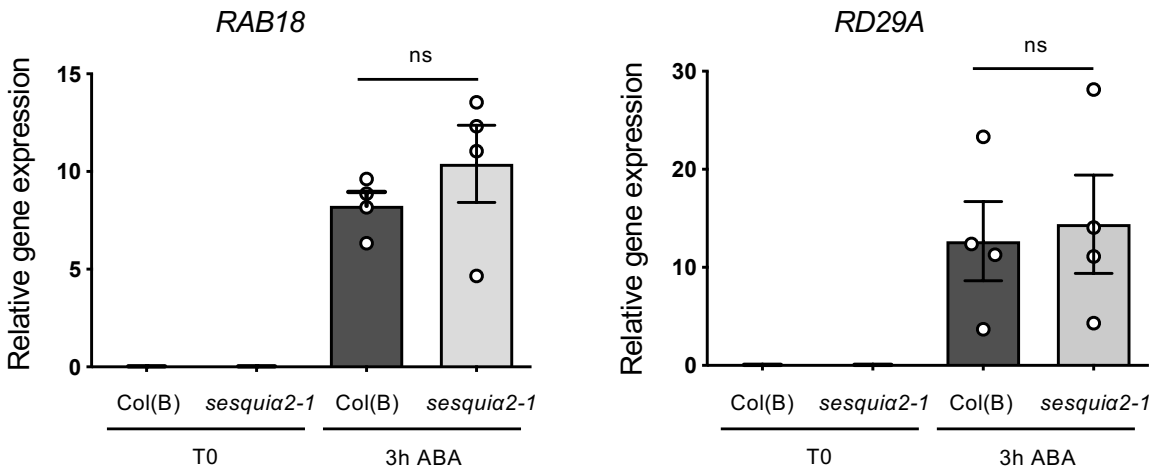

Supplementary Figure 6

a

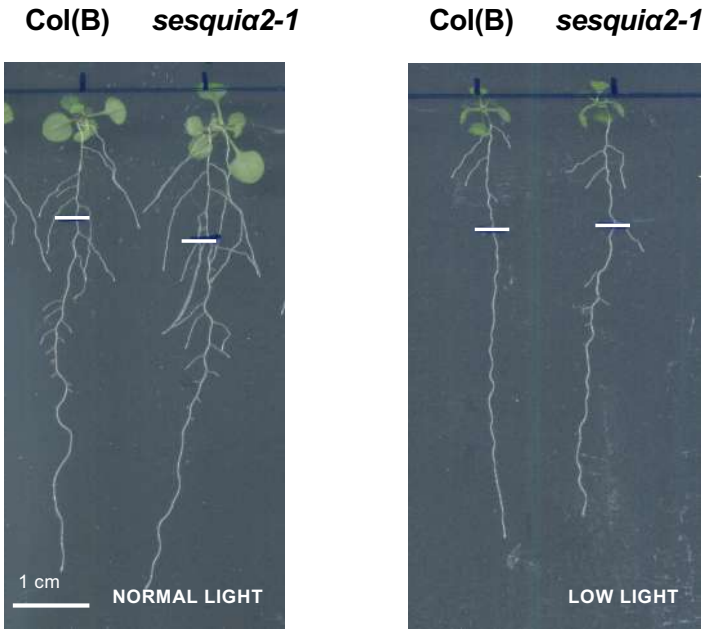

b

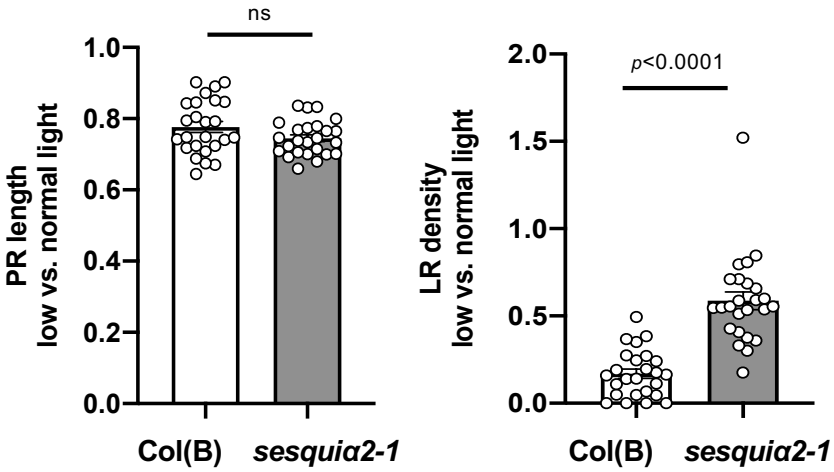

Supplementary Figure 7

a

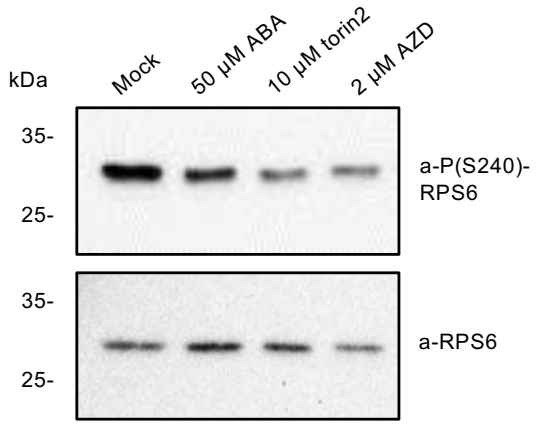

b

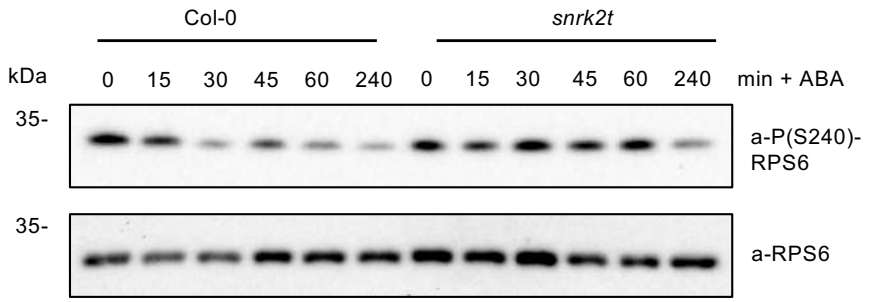

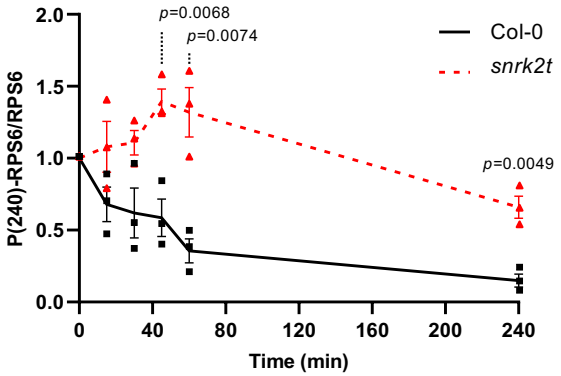

Supplementary Figure 8

a

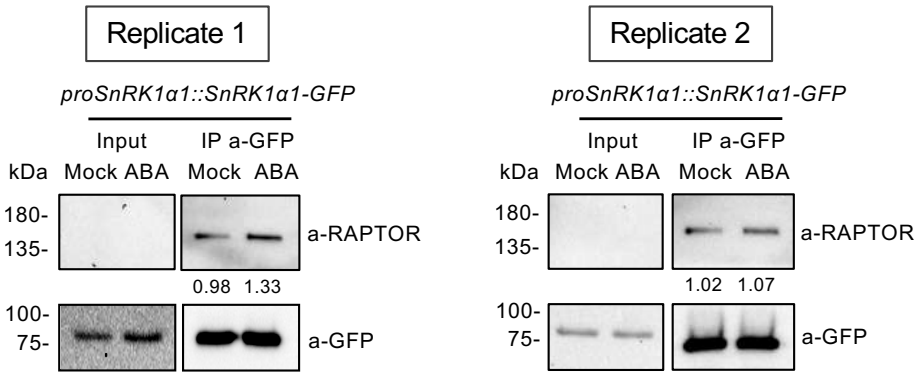

b

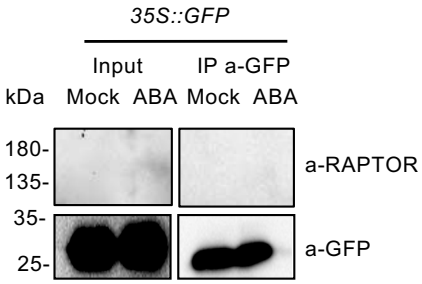

c

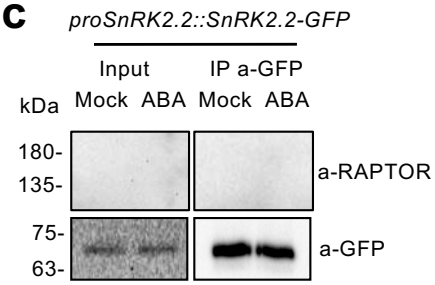

d

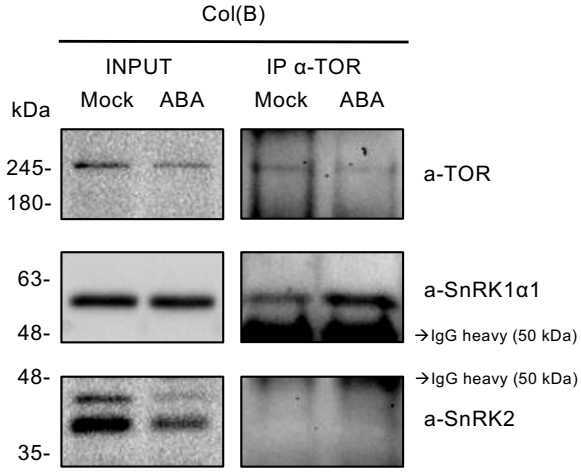

Supplementary Figure 9

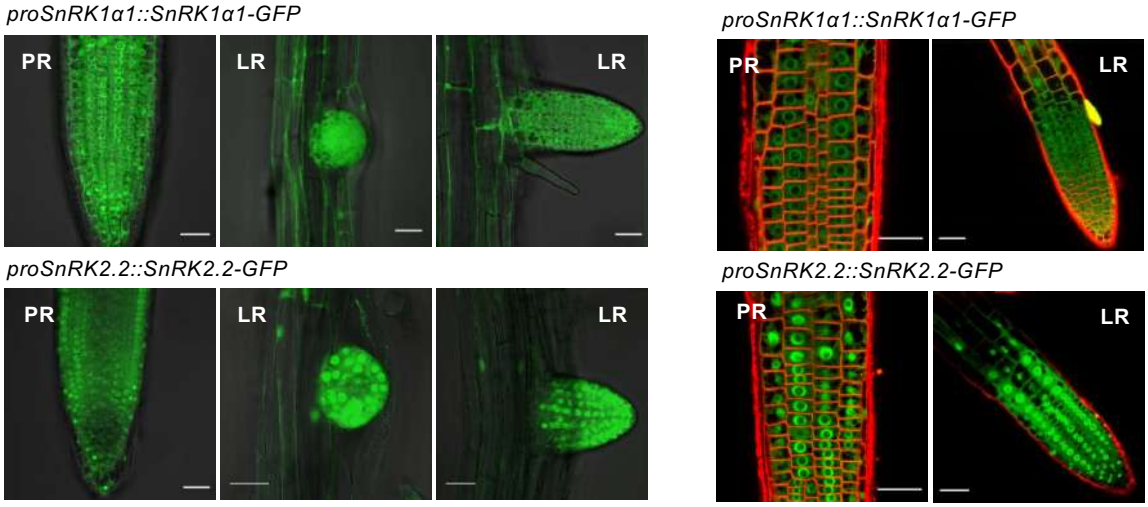

Supplementary Figure 10

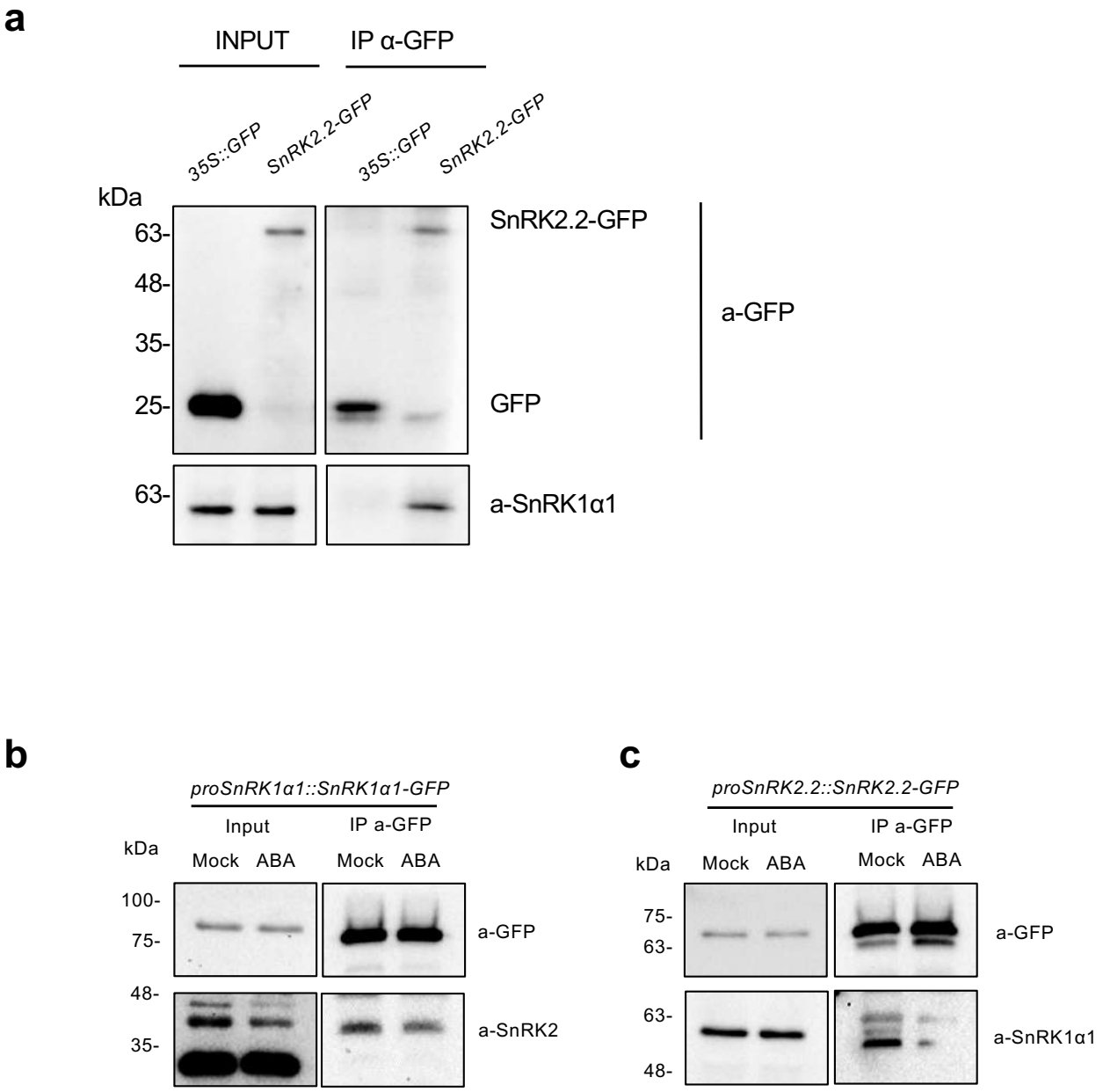

Supplementary Figure 10 (continued)

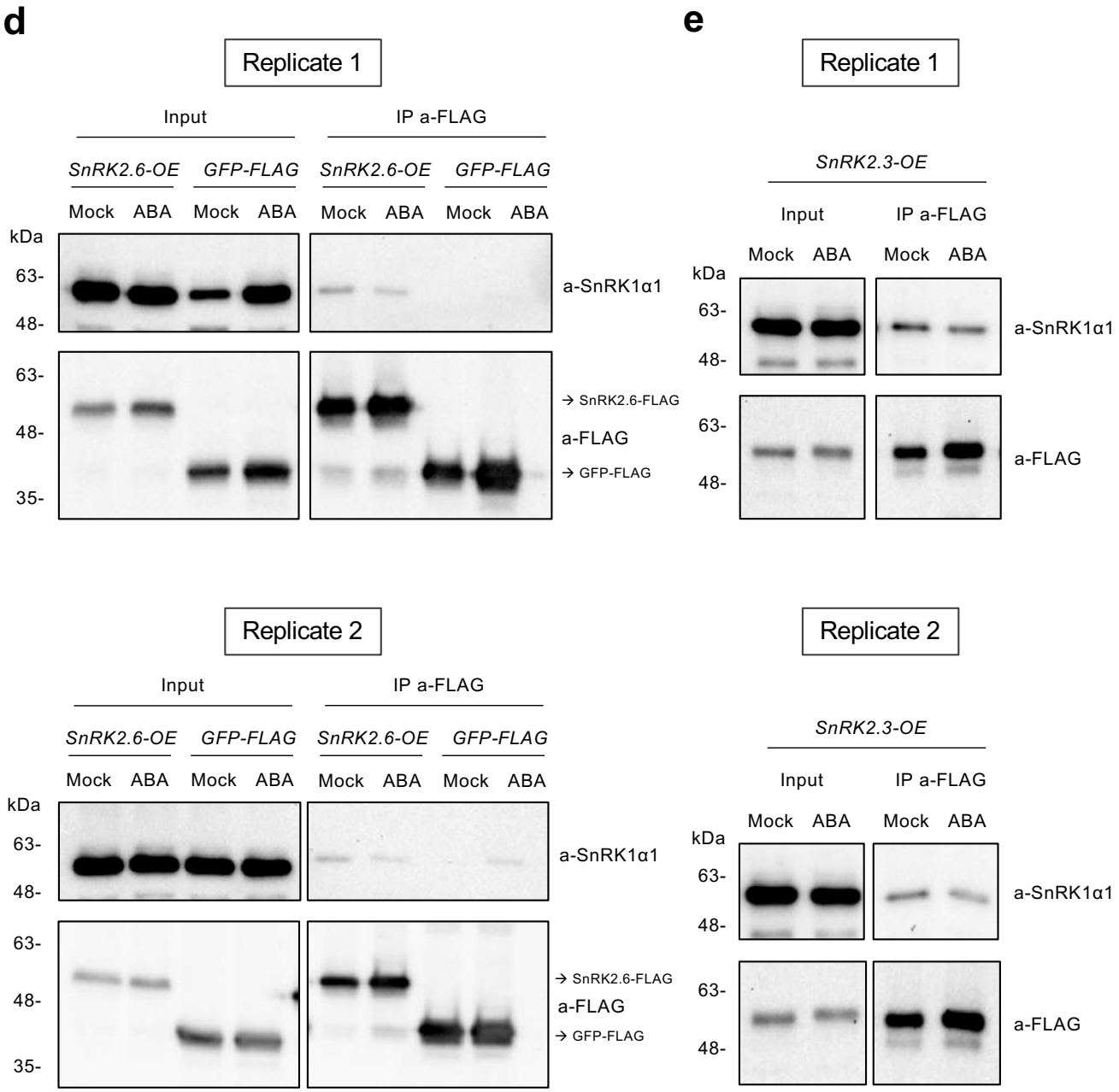

Supplementary Figure 11

a

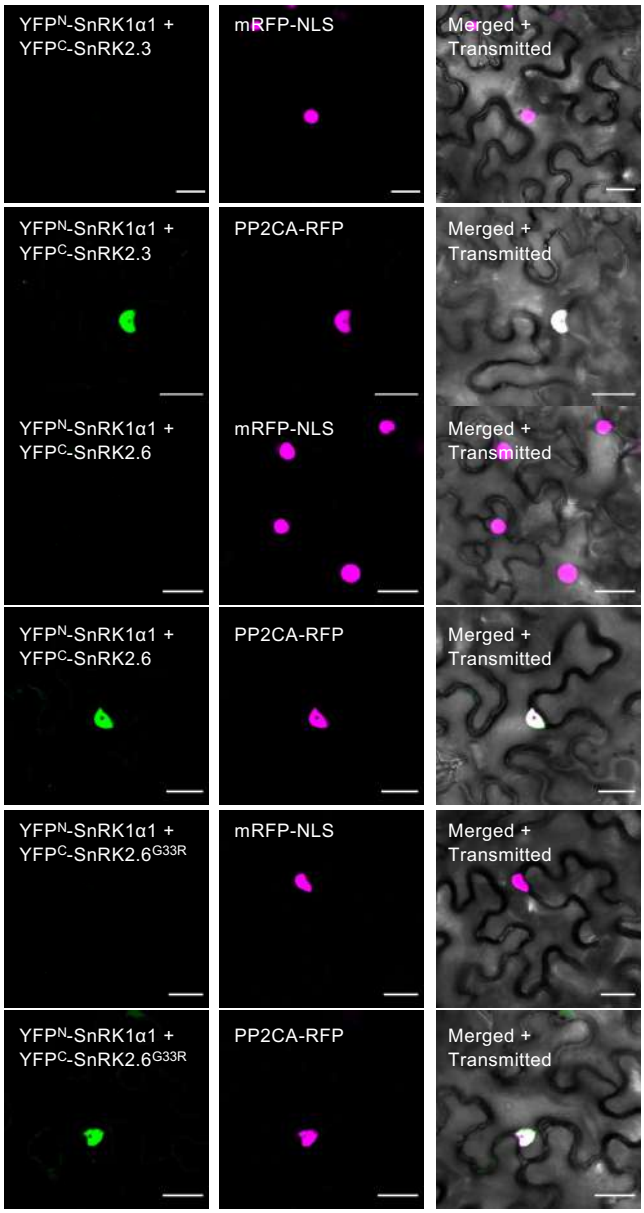

b

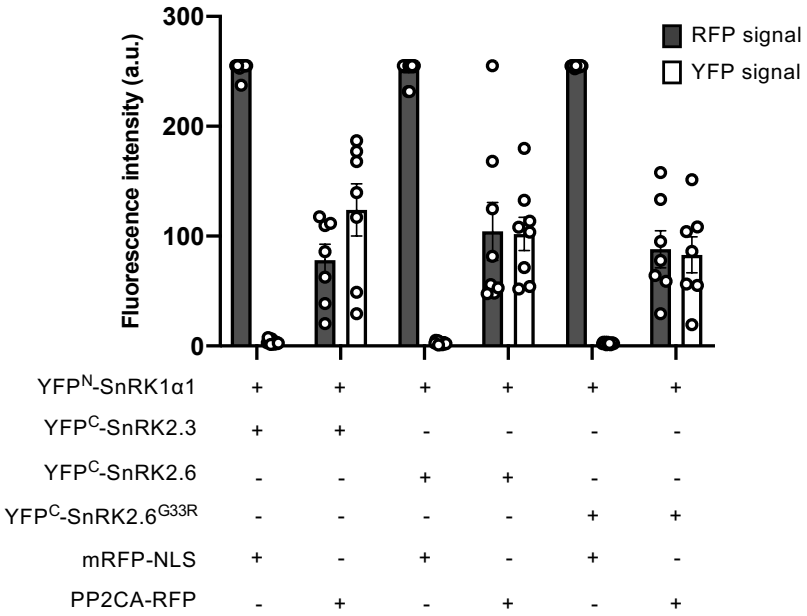

Supplementary Figure 11 (continued)

c

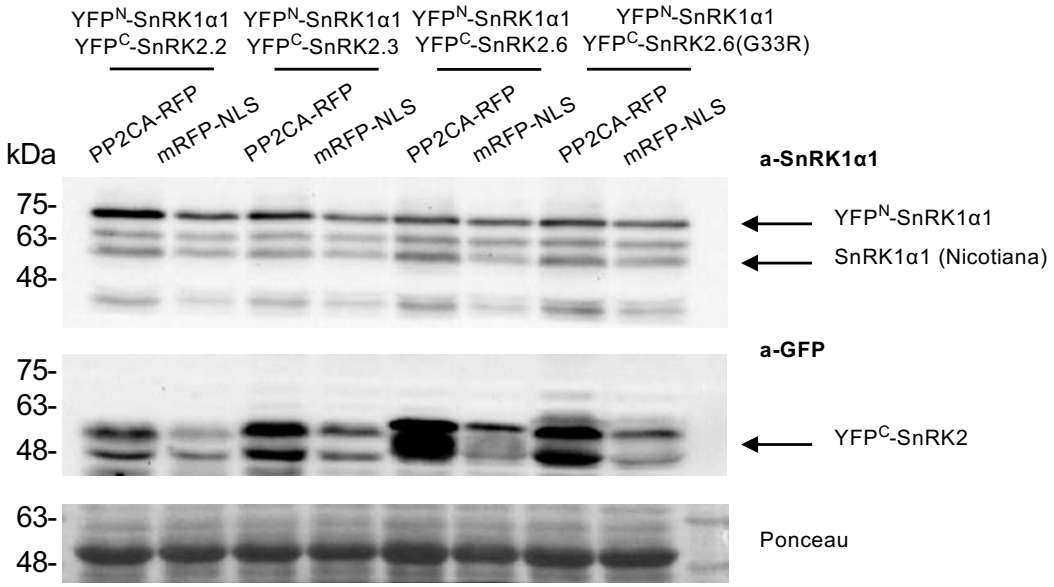

Supplementary Figure 12

a

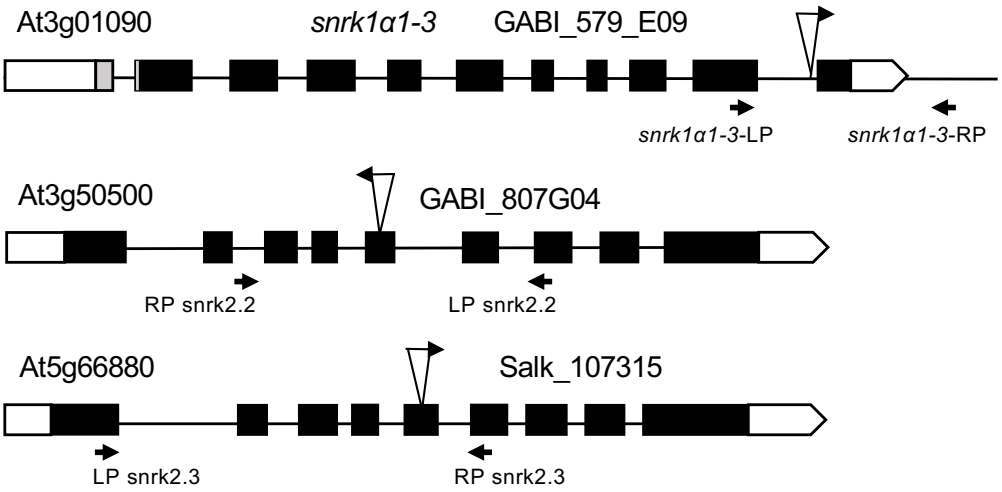

b

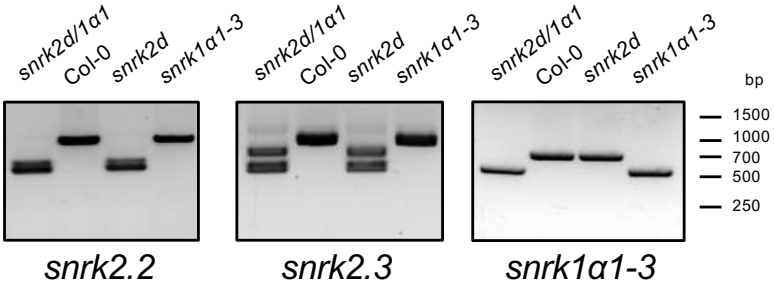

Supplementary Figure 13

a

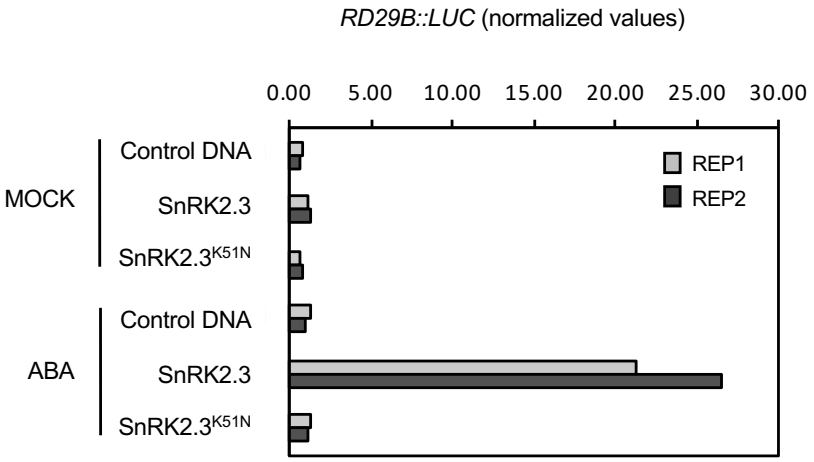

b

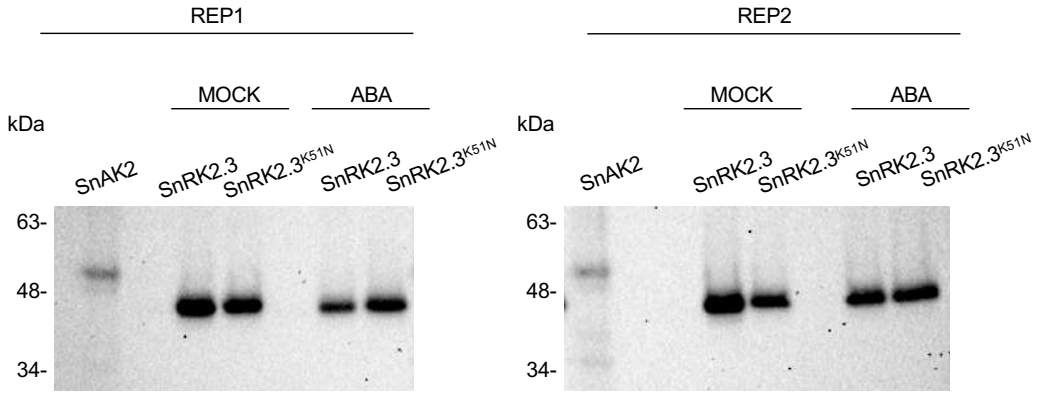

c

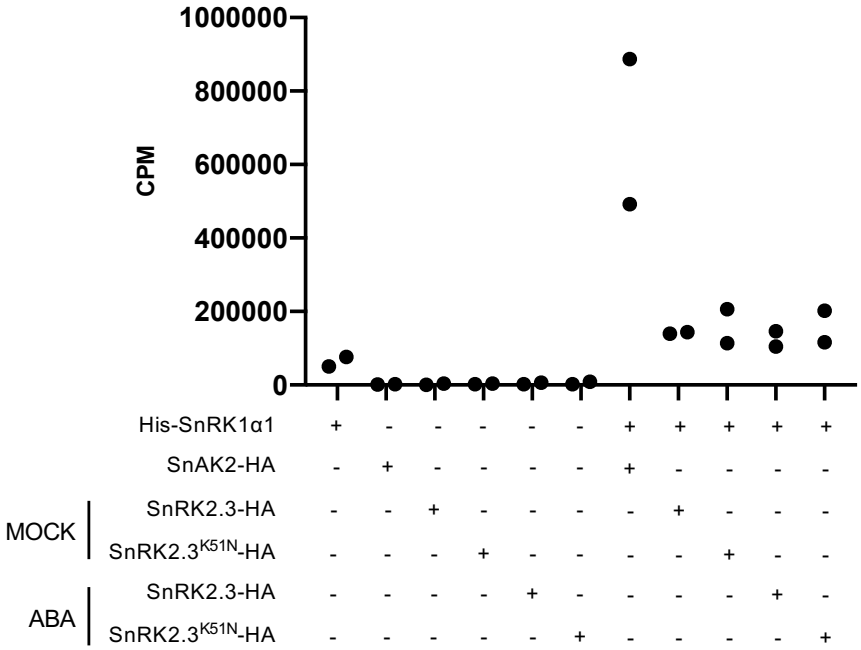

Supplementary Figure 14

a

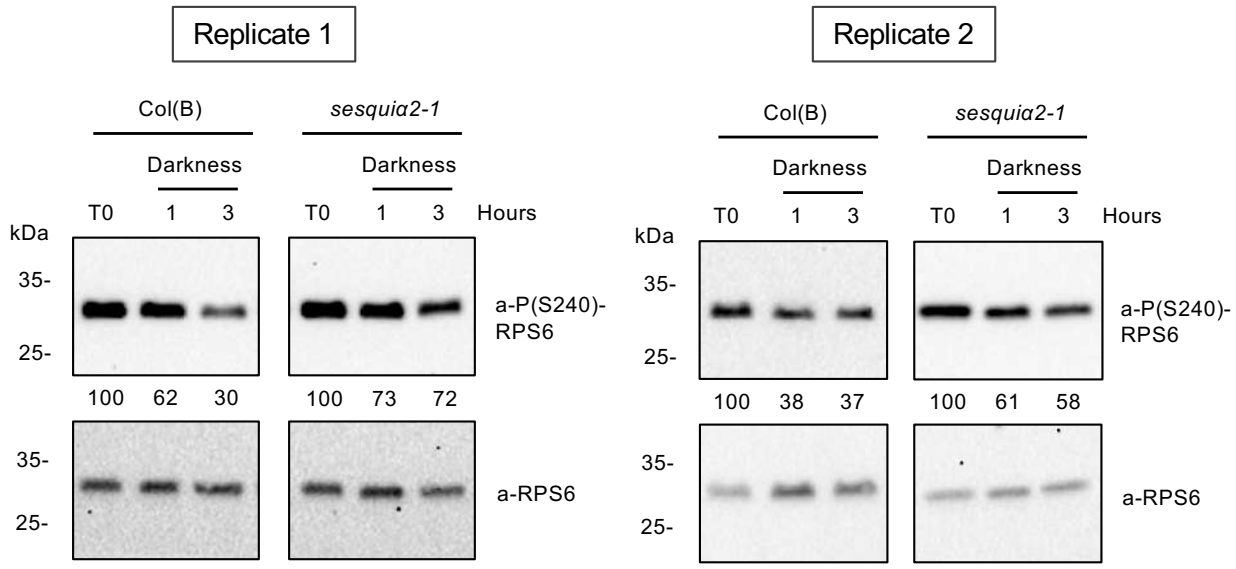

b

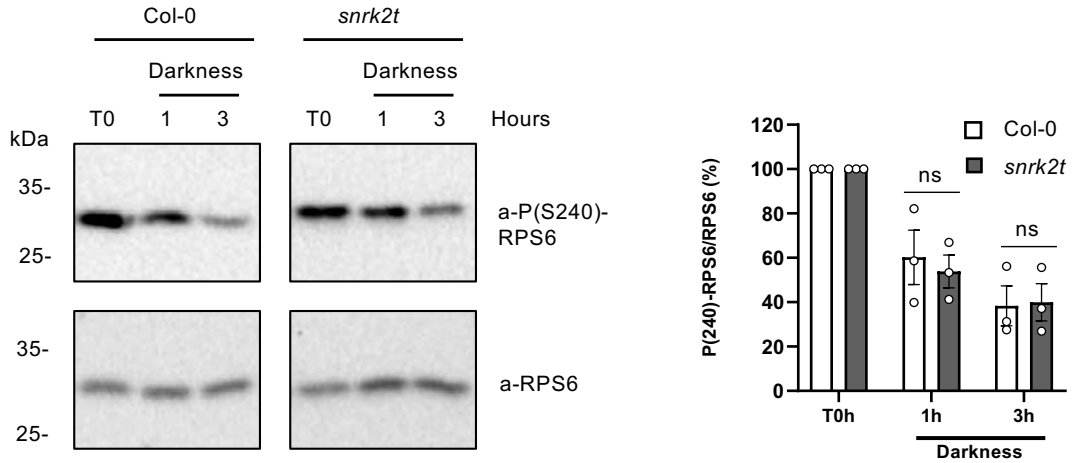

Supplementary Figure 15